FEDERAL COMMUNICATIONS COMMISSION

FOPSI PROJECT

REPORT ON PHASE

HYBRID ANALYSIS OF INTERCEPTION DATA

Reproduced by
NATIONAL TECHNICAL
INFORMATION SERVICE
Springfield, Va. 22151

RESEARCH DIVISION
OFFICE OF THE CHIEF ENGINEER
FEDERAL COMMUNICATIONS COMMISSION
WASHINGTON, D.C. 20554

September 15, 1970

THIS DOCUMENT HAS BEEN REPRODUCED
FROM THE BEST COPY FURNISHED
US BY THE SPONSORING AGENCY

DISCLAIMER NOTICE

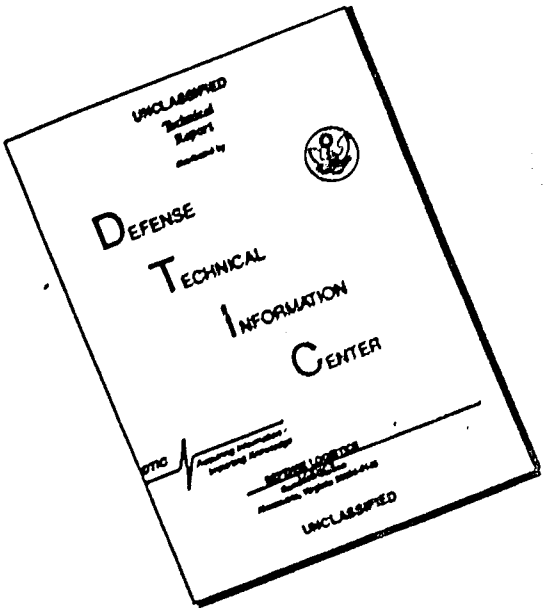

THIS DOCUMENT IS BEST QUALITY AVAILABLE. THE COPY FURNISHED TO DTIC CONTAINED A SIGNIFICANT NUMBER OF PAGES WHICH DO NOT REPRODUCE LEGIBLY.

Federal Communications Commission
Office of Chief Engineer
Research Division

Report No. R-7003

December 15, 1970

FCC/USAF POPSI PROJECT

Detailed Analyses of Precipitation Data

By

Roger B. Carey
Gary S. Kalagian

Washington, D. C.
20554

SUMMARY

The electromagnetic field strength measurements ~~($\lambda = 5.2$ cm.)~~ obtained during the 1966 FCC/USAF POPSI Project have been classified according to propagation mode and the data from periods of precipitation have been analyzed in detail. Cumulative probability distributions were generated for the effective radar reflectivities derived from the bistatic electromagnetic measurements and compared with the probability distributions of the surface rainfall rates derived from the accumulations of the United States Weather Bureau recording rain gauges in the area. The distribution functions were then adjusted by means of a least squares regression line to obtain a $Z(p) - R(p)$ relationship for effective reflectivities in excess of 10^6 mm $^6/m^3$ and surface rainfall rates up to 105 mm/hr. The relationship thus obtained has been compared with other Z-R relationships based upon the analysis of drop size distributions and has been tested against independent rain gauge data in the POPSI Project area. The final approximation resulted in a standard deviation for estimating $Z(p)$ from $R(p)$ of less than 1.6 dB for the New Jersey rainfall data, and appears to be more representative ~~than $Z = 200R^{1.6}$~~ for the actual relationship between $Z(p)$ and $R(p)$ for convective storms. The altitude dependence of the reflectivity from precipitation-connected phenomena in the New Jersey coastal area has been demonstrated and discussed to some extent.

CONTENTS

1.0	Introduction
2.0	Separation and Grouping of Data
3.0	Contemporary Theory
4.0	POPSI Project Detailed Analysis Technique
5.0	Correlation of Z and R by Data Time Periods
6.0	Z-R Relationship by Correlation of Probability Distributions
7.0	Altitude Dependence of the Effective Reflectivity of Severe Convective Storms
8.0	Modification of the Z-R Relationship to Accomodate the High Reflectivities of Severe Convective Storms
9.0	The Effect of Rainfall Integration Interval Upon the Probability Distribution Function
10.0	Conclusions
11.0	Acknowledgements
12.0	Bibliography

Index to Figures and Tables

Figure No.

1 POPSI Project Meteorological Facilities.
2 Z (Max.) versus R (Max.) - 1 hour accumulations.
3 Z (Max.) versus R (Max.) - 15 minute accumulations.
4 Z versus R - October, 1966.
5 Probability Distributions - R from 15 minute accumulations of U.S.W.B. rain gauges, R calculated from measured Z by using relationship $Z = 200R^{1.6}$.
6 R(p) versus Z(p) by altitude of common volumes.
7 Z versus Height of CV, NAFEC & WW, 6/28/66. 1700-1800 hours.
8 Z versus Height of CV, NAFEC, 6/28/66, 1500-1600 and 1800-1900 hours.
9 Z versus Height of CV, WW, 6/28/66, 1500-1600 and 1800-1900 hours.
10 Recorder Charts - Fading Rate during Precipitation.
11 Refractive Index Profile, NAFEC, 6/28 - 1410.
12 Refractive Index Profile, JFK, 6/28 -1215.
13 Refractive Index Profile, JFK, 6/28 - 1815.
14 PPI Scope Photographs, NAFEC WSR - 57, 6/28, 1515-17.
15 PPI Scope Photographs, 6/28, 1632.
16 PPI Scope Photographs, 6/28, 1708-10.
17 Correlation of Altitude of Maximum Z and 0° Isotherm (Melting Layer).
18 Equivalent Reflectivity/Rainfall Rate (Z/R) Relationship Derived from Probability Distributions of POPSI Field Strength Measurements and Precipitation Accumulations of U.S.W.B. Recording Rain Gauges.
19 Probability Distributions -15 minute and 1 hour accumulation periods of POPSI rain gauges and 1 hour periods of independent rain gauges.
20 Equivalent Reflectivity/Rainfall Rate (Z/R) Relationships Derived from Probability Distributions of POPSI Field Strength Measurements and Precipitation Accumulations of POPSI and Independent Rain Gauges.

Table No.

I Sample Populations (number of samples, altitude groups, effective reflectivities).
II Z(p) - R(p) Regression Lines - Goodness of fit.
III Summary of Test of Z - R Relationships.

1.0 INTRODUCTION

During the period from 15 February 1966 to 16 February 1967, the FCC and USAF, with the cooperation of the U. S. Coast Guard, the FAA, the U. S. Weather Bureau, and NASA, conducted an investigation of the signal power scattered from precipitation and other mechanisms in the common volumes established by the intersections of the beams from transmitting antenna operating in a configuration simulating a satellite earth station and receiving antennas configured in a manner typical of terrestrial microwave radio-relay stations. The investigation was conducted at a radiation wavelength of 5.21 centimeters (5.75 GHz) in an area near the New Jersey Coast and was designed to obtain data for a statistical treatment of the scattered interference problem. The details of this POPSI (Precipitation and Off Path Scattered Interference) Project may be found in FCC Research Division Report No. R-6801, dated 15 March 1968.(1)

In the period immediately following the FCC/USAF project, several domestic and international groups were convened for the purpose of agreeing upon the form and direction of research projects to further the investigation of the off-path propagation phenomena and to derive allocation criteria which would recognize the interference potential to terrestrial microwave and satellite communication system earth stations. However, it was not until midway through fiscal year 1970 that a project was initiated under the management of a U. S. interagency group (2). Meanwhile, the FCC Research Division decided to proceed with a detailed analysis of the original POPSI Project data.

2.0 SEPARATION AND GROUPING OF DATA

Although the original objectives of the POPSI Project did not include the positive identification of the dominant propagation mechanism at all times, the raw data records and meteorological data inputs were adequate to permit a computerized format for the identification of the predominant propagation mode during certain specific time periods.

Without going into detail, the tools used for propagation mode identification included:

a. Comparison of the medians of simultaneous 5-minute intervals of the great-circle and off-path signals, and correlation of the differences with known antenna side-lobe radiation patterns.

b. Chart recordings from the U. S. Weather Bureau rain gauges in the vicinity of the propagation paths.

c. Vertical profiles of humidity, temperature and refractive index gradients constructed from radiosonde data taken every four hours from a location near the transmitter site and intermittently from a location on the great-circle path.[3, 4]

d. Time-lapse photographs of the PPI scope of a WSR 57 weather radar located on the great-circle path.[5, 6, 7, 8, 9]

e. Correlation of the short-term variability (fading rate) of the off-path signal with that of the great-circle path signal.[10, 15, 54]

For the detailed analyses, the data were divided into hourly segments and assigned to one of three groups, according to the propagation mode.

1. Precipitation Scattering

2. Guided Propagation (ground-based and elevated layer ducting).

3. Mixed (combination of precipitation scattering and guided propagation).

Very few difficulties were encountered in the identification and analysis of off-path signal enhancements attributed to precipitation alone, and the periods of ground-based ducting were easily recognized. However, severe problems in identification and analyses were experienced with the high signal levels associated with elevated temperature inversions or humidity lapses in the absence of measurable surface precipitation and with the directional, partially-coherent, propagation often associated with precipitation from a heavily stratified troposphere.[11, 55, 56] The analysis of this "mixed mode" propagation has been difficult because of insufficient meteorological input, unfavorable path geometry, and the lack of an adequate model.

3.0 CONTEMPORARY THEORY

The scattering and attenuation of electromagnetic waves by particles in the atmosphere are complex functions of the particle size, dielectric properties, and the radiation wavelength.[12, 13, 14] The theoretical treatment of the relationships among forward-scattered power, back-scattered power, radar reflectivity, back-scattering cross-section, and rainfall rate, are usually simplified by beginning with the Rayleigh approximation for the back-scattering cross-section of a single spherical particle (raindrop, ice particle, hailstone, etc.) having a diameter, D. This cross-section is

$$\sigma = \frac{\pi^5 |K|^2 D^6}{\lambda^4} \qquad (3\text{-}1)$$

where K is a function of the particle refractive index, and λ is the radiation wavelength. Equation (3-1) is generally considered to be valid when $\pi D/\lambda \leq 0.2$. In this special case, the back-scatter is proportional to $|K|^2$ where

$$K = \frac{m^2 - 1}{m^2 + 2} \tag{3-2}$$

m is the square root of the complex dielectric constant, ϵ, and is equal to $n-j\kappa$ where n is the phase refractive index and κ is the absorption coefficient of the particle substance. Although the experimentally-derived values of n and κ have exhibited some dependence upon temperature and wavelength, the variations in the centimetric band appear to be slight and $|K|^2$ is usually assumed to be 0.93 for water and 0.176 for ice.

For N particles per unit volume, the back-scattering cross-section per unit volume (reflection coefficient) is

$$\eta = \Sigma\sigma = \frac{\pi^5 |K|^2 \Sigma ND^5}{\lambda^4} \tag{3-3}$$

If all the particles are assumed to be the same size, the quantity known as the equivalent reflectivity, Z, is expressed by

$$Z = \Sigma ND^6 \tag{3-4}$$

If the particles are not the same size but instead have a "drop size distribution,"

$$Z = \sum_{i=1}^{n} N_i D_i^6 \tag{3-5}$$

In any event, equation (3-3) becomes

$$\eta = \frac{\pi^5 |K|^2 Z}{\lambda^4} \tag{3-6}$$

It can be seen from equations (3-3), (3-4), and (3-5) that the particle diameter is, by several orders of magnitude, the most significant parameter in the determination of Z, and hence the determination of R by the indirect method (conversion of surface rainfall rate to reflectivity factor, Z, or to reflection coefficient, η).

Nearly all recent investigators are agreed that there appears to be no unique drop-size distribution for a given rainfall rate R; therefore, there can be no unique relationship between Z and R. (17, 18, 19, 20, 21, 22, 23, 24) However, in considering the effect of precipitation-scattered interference upon satellite and terrestrial microwave communications systems, the use of empirical relationships between effective radar reflectivities and nearby surface rainfall rates is especially attractive, inasmuch as the probability distribution functions of surface rainfall rates are parameters that can be derived from meteorological records available in a large part of the world.[25] Most of the relationships between effective reflectivity and surface rainfall are of the form

$$Z = aR^b$$

where Z is the effective reflectivity and R is the surface rainfall rate. The empirical constants are a and b. One of the most popular of the relationships was derived from the application of the Rayleigh particle scattering theory to the observed drop size distributions for various rainfall rates

$$Z = 200\ R^{1.6} \qquad (3\text{-}7)$$

where Z is in $mm^6\ m^{-3}$ and R is in mm/hr. The reflection coefficient, η, may also be determined, more or less, from actual electromagnetic wave propagation measurements by using the relationship,

$$\eta = \frac{(4\pi)^3 P_r (d_r d_t)^2}{P_t G_t G_r\ \lambda^2 V} \qquad (3\text{-}8)$$

where P_r = power at receiver input terminals.

P_t = power at transmitter output terminals.

G_t, G_r = transmitting and receiving antenna gains (over isotropic).

λ = radiation wavelength.

d_t = distance from transmitter site to scatterer.

d_r = distance from receiver site to scatterer.

V = common volume.

Actually, equation (3-8) is a re-arrangement of the bi-static radar equation, which is in turn a slight modification (2 distances instead of 1; 2 antenna gains instead of 1; and pulse length instead of 1/2 pulse length) of the radar back-scatter equation. Implicit in the use of (3-8) for a forward-scatter solution is the assumption that the scattering is isotropic or exhibits insignificant anisotropy. It is a scalar formula and can be used only to obtain values of η or Z if they are also scalar functions.* (26, 27, 28)

4.0 POPSI PROJECT DETAILED ANALYSIS TECHNIQUE

After grouping the data as described in section 2.0 and eliminating the direct-path signal components, the medians of the five minute power inputs recorded by the off-path receivers were coupled with the system parameters to calculate the effective reflectivities for each common volume configuration by using the equations, (3-8) and (3-6).

$$\eta = \frac{(4\pi)^3 P_r (d_t d_r)^2}{P_t G_t G_r \lambda^2 V} \qquad (3\text{-}8)$$

$$Z \text{ (eff.)} = \frac{\lambda^4 \eta}{\pi^5 |K|^2} \qquad (3\text{-}6)$$

---

* / For the prediction of interference to services having high reliability criteria, the infrequent but extremely high signal levels exhibiting directional, partially coherent characteristics should be considered, although the number of parameters in the explanatory theories is almost prohibitive. Nearly all of these theories involve vector approaches, such as geometrical optics approximations or quasi-exact solutions of the wave equations. In fact, even the scattering theory, when larger particles are involved ($\frac{\pi D}{\lambda} > 0.2$), forces exact solutions of the Mie equations. A large segment of the POPSI Project data fall in this category but the analysis was considered to be beyond the scope of this report.

where the parameters are as previously indicated except that, in this case,

d_t = distance from transmitter site to center of common volume

d_r = distance from receiver site to center of common volume

V = common volume defined by antenna beam half-power points and pulse length

$|K|^2$ = 0.93

Equation (3-7) was then used to normalize the effective reflectivity to the apparent rainfall rate in mm/hr.**

$$Z = 200\ R^{1.6} \qquad (3\text{-}7)$$

The rainfall rates were derived from the accumulations recorded by U. S. W. B. rain gauges at NAFEC, Cape May, Glassboro, Freehold, Hightstown, Lumberton, and Marlton, New Jersey. The locations of the POPSI Project common volumes with respect to the rain gauges are shown on Figure 1. The MESONET stations in the NAFEC area are also identified, although technical problems dictated against the use of precipitation data from them in the final analysis.(30) The rain gauge recorder charts were rather difficult to analyze but could generally be interpreted to within .01 of an inch for each 15-minute interval. For purposes of analysis,

$$\text{Precipitation Rate: } R(\text{mm/hr.}) = 100\ A \qquad (4\text{-}1)$$

where A = hundredths of an inch accumulated during each 15-minute period beginning on the hour, quarter-hour, half-hour, etc.

This rate was then assumed to be constant during the entire 15-minute period.

** /Although this was done only for comparison purposes, it is a common procedure in calculating rainfall rates from radar returns.(31, 35, 58) However, it may not always be a valid procedure due to the statistical manner in which the Z-R relationship was obtained. The form of $Z = 200\ R^{1.6}$ implies that it was the best fit for a regression line of the dependent variable, log Z upon the independent variable, log R. Although the variables can be interchanged, the best fit regression line may not be the same. Futhermore, the greatest deviation could be expected at the high reflectivity extremes of the regression lines. (29)

5.0 CORRELATION OF Z WITH R BY DATA TIME PERIODS

Point-by-point correlation of measured rainfall rates with those calculated from the scattered electromagnetic field introduces certain requirements. (32, 33, 34, 35) In addition to exact time-frame synchronization, the rain gauge system aperture should be equated with that of the common volume to avoid undesirable averaging. Futhermore, the rain gauge field should be properly located with respect to the common volume. None of these requirements are likely to be met by any significant research program or as boundary conditions for an allocation model. Figure 1 indicates that the POPSI Project was certainly no exception in these respects although the recording rain gauge facilities were as extensive as can reasonably be expected outside of the concentrated, special-purpose networks being operated in a few limited areas. (57,36) Real time correlation cannot be expected between the ground based rain gauges and effects in the common volumes, since the gauges are displaced from the common volumes both horizontally and vertically. Although in most areas it can be expected that the statistics of rainfall on the ground may be very similiar to those in the common volume, the rainfall occuring here, at varying altitudes during a scattering event may bear no relation to the rainfall measured at a gauge on the earth's surface. Further, it should be noted that there are areas of the country where "dry" thunderstorms are common. In this event rain or hail can be present in the common volume with a complete absence of precipitation on the ground.

Although the possiblity of acceptable short-term Z-R correlation seemed to be remote because of the ambiguities introduced by space and time differences between the meteorological and the electromagnetic data inputs, some effort was made in this direction. For both 15-minute and one hour periods the effective equivalent reflectivities were calculated from the highest median power of the five minute samples during the interval. If the rainfall rates derived from the maximum accumulations in the rain gauge system during the same periods were at least one mm/hr.*, they were paired with the corresponding reflectivities to obtain the scatter diagrams of Figures 2 and 3.

The effective equivalent reflectivities as calculated from equations (3-6) and (3-8), and the rainfall rates derived from the rain gauge accumulations, were assumed to be related by the form, (16)

$$Z = aR^b$$

---

* / The minimum requirement of 1.0 mm/hr. in the rain gauge system, regardless of the corresponding reflectivities, resulted in the removal from consideration of more than half of the data including 13 of the highest effective reflectivities ($Z \geq 10^5$).

where a and b are constants. By the logarithmic transformation the form becomes linear with log Z as the dependent variable, and log R as the independent variable. Since a number of proposals have been advanced for predicting "Z" values from "R" values measured at the surface, the least squares regression lines of log Z upon log R for the scatter diagrams are of interest. These have been calculated and are shown on the diagrams along with the loci of other empirical relationships of the same form. If the relationship between "Z" and "R" were nearly linear or if the data points were evenly distributed across the interval of consideration, the least squares regression lines of Figures 2 and 3 might be useful for rough prediction on a point-by-point basis. However, the relationship, instead of being linear, is in the form of a geometric curve with the bulk of the points at the lower reflectivity values which are of little interest and where the bivariate distribution is truncated with respect to rainfall rates. This results in a least squares regression line which is heavily biased by data of no real importance. It is interesting to note that the hourly data shows significantly better correlation than the 15-minute data. This was expected because of the averaging involved. Data for periods longer than one hour would probably be better correlated and the correlation of instantaneous Z/R data would probably be almost nil.

<u>Hourly Data</u>

Least squares fit:	$Z = 431.9\ R^{.563}$
Coefficient of correlation:	.34086
Standard error of estimate:	6.5 dB
(Maximum Z from maximum R):	
Standard error of estimate: (Using $Z = 200\ R^{1.6}$)	8.2 dB
Standard error of estimate: (Using $Z = 127.7\ R^{2.26}$)	10.5 dB

<u>15-minute Data</u>

Least squares fit:	$Z = 431.2\ R^{.297}$
Coefficient of correlation:	.17714
Standard error of estimate:	7.2 dB
Standard error of estimate: (Using $Z = 200\ R^{1.6}$)	9.8 dB
Standard error of estimate: (Using $Z = 127.7\ R^{2.26}$)	12.3 dB

The futility of point-by-point correlation of reflectivities with nearby surface rainfall rates is emphasized by Figure 4, a scatter diagram of the data for October. The refractive index profiles for this period indicated very little low-level atmospheric stratification and the surface rainfall rates appeared to be uniform over a large area. Theoretically, this period should promise the best Z-R correlation for heavy rainfall rates. Actually however, the correlation was quite poor with reflectivities generally lower than would be expected from the corresponding surface rainfall rates. This may have been caused by common volumes which were above the 0°C. altitude level and confined to an area that was quite small compared to the rain gauge system aperture.

6.0 Z - R RELATIONSHIP BY CORRELATION OF PROBABILITY DISTRIBUTIONS

Since it has been implicitly assumed that Z and R are related, their probability density functions must also be related if they have been determined from data extending over the same time frames and confined to the same synoptic weather prediction area. This appears to be the best approach to the problem of Z-R correlation, since the effects of the real time and space differences between the meteorological and the electromagnetic data inputs are minimized.

Precipitation rates derived from the 15-minute accumulations of rain gauges in the U. S. W. B. system were used to generate a cumulative probability distribution. The data from all of the gauges were grouped together for periods during which the transmitter and at least one off-path receiver were in operation. This distribution involved over 87,000 15-minute samples extending from February through October, and includes derived surface rainfall rates up to 105 mm/hr. This probability distribution is specifically indicated on Figure 5 and is represented by a smooth curve on Figure 6. The effective reflectivities were calculated in accordance with section 4.0 and used to generate probability distributions by common volume groups as indicated in Table 1. These probability distributions are shown in Figures 5 and 6. In these Figures the ordinate values for Z have been normalized to the rainfall rate, R, by using the relationship, $Z = 200\ R^{1.6}$. In the interval, $40 \leq R \leq 100$ (mm/hr.), the distribution function for the 15-minute rainfall rates compares quite favorably with what a recent investigator derived for the instantaneous rates in dense rain gauge systems in the same area (36).

Upon examination of Figures 5 and 6 it is apparent that the relationship between the distribution function of the effective reflectivities and that of the surface rainfall rates is somewhat dependent upon the common volume altitude. This dependence is not significant at rainfall rates of less than 10 mm/hr. or with

common volumes below an altitude of two kilometers. These same boundary conditions might be considered to be descriptive of the widespread uniform precipitation associated with frontal or orographic lifting and common to temperate climates in early spring and late fall. For this type of precipitation, the relationship between Z and R or, more specifically, the relationship between Z(p) and R(p) can be approximated by the expression: $Z = 200\ R^{1.6}$. There is also evidence that, for a climate similar to that of the New Jersey coast, the elimination of common volumes in the 2 to 5-kilometer altitude bracket would extend the usefulness of the $Z = 200\ R^{1.6}$ approximation to somewhat higher rainfall rates.

7.0 ALTITUDE DEPENDENCE OF THE EFFECTIVE REFLECTIVITY OF SEVERE CONVECTIVE STORMS.

The altitude dependence of the effective reflectivity of severe convective storms has been well documented in the literature.(8, 37, 38,39). Several of these storms passed through the propagation path area during the period of the POPSI Project but only one of them has been analyzed in detail. This storm occurred on 28 June 1966 and, although not accompanied by extremely heavy surface rainfall resulted in effective reflectivities in the order of 10^6 mm $^6m^{-3}$. The altitude intervals and magnitudes of the reflectivities noted in connection with this storm are shown in Figures 7, 8, and 9. Because the common volume samples were selected at random rather than as a result of probing the storm for reflectivity, the actual maximum reflectivities existing in the cells may have been somewhat higher than indicated. During this storm the fading rate (Figure 10), the refractive index profiles (Figures 11, 12, and 13) and the photographs of the PPI scope of the WSR 57 radar at NAFEC (Figures 14, 15, and 16) clearly indicate precipitation scattering as the mode of propagation. From the time the front entered the U.S.W.B. rain gauge system at 1100 hours until its departure at 2100 hours, the maximum rainfall rate derived from any of the rain gauge samples was 60 mm/hr. and from the entire network of seven gauges there were only seven 15-minute samples that indicated surface rainfall rates in excess of 20 mm/hr. The high reflectivites which persisted for some time were probably due to hail aloft, although very little of it reached the ground. The "fingered" appearance of the storm cells on the PPI scope photographs and the extremely high "radar tops" as noted by the NAFEC weather radar operator (over 17 kilometers) indicated the presence of large hailstones in this storm.(40, 41, 42, 43, 44, 45)

Since the convective storms are the principal contributors to the high reflectivity portion of the probability distribution function for precipitation scattering, and exhibit the greatest disparity between reflectivity aloft and nearby surface rainfall

rates, they must be taken into account in the consideration of possible interference to high-reliability services. It is possible that the effect of these storms can be accomodated by a suitable modification of an empirical Z-R relationship or by "blocking" the troublesome altitude interval to common volumes for allocation purposes or by introducing some other altitude-discriminant meteorological parameter such as the "melting level" or 0°C. isotherm. The somewhat complicated chart exhibited in Figure 17 represents an attempt in this direction.

8.0 MODIFICATION OF THE Z-R RELATIONSHIP TO ACCOMODATE THE HIGH REFLECTIVITIES OF CONVECTIVE STORMS.

As previously pointed out, the elimination of common volumes in the two to five kilometer altitude interval in the New Jersey area would extend the usefulness of the $Z = 200\ R^{1.6}$ approximation to the point where an acceptable level of precipitation scattered interference could be predicted from the surface rainfall rate probability distributions. However, when the interference probability prediction was extended to $p \leq .0005$, without regard to common volume altitude, the application of the $Z = 200\ R^{1.6}$ approximation resulted in estimates of Z from R(p) approximately 10 dB below those indicated by the New Jersey measurements.

By adjusting the rainfall rate distribution function to fit the measured Z distribution function at points of equal probability it was possible to arrive at a Z(p) - R(p) relationship which more nearly describes that of the New Jersey data. This adjustment was accomplished by the least squares fit of the regression line

$$\log Z(q) = \log a + b \log R(q) \qquad (8\text{-}1)$$

where $q = p(R)$ for $1.0 \leq R \leq 105$ mm/hr.

The relationship obtained in this manner was

$$Z(p) = 127.7\ R(p)^{2.26} \qquad (8\text{-}2)$$

and is shown in Figure 18 along with the regression line represented by $Z = 200\ R^{1.6}$ and some recent Z-R relationships from the dense Illinois rainfall survey system.[46] The trend of the Z values in the neighborhood of 10^6 indicates that even this new relationship would probably result in the underestimation of Z (effective) for the high moisture content zones of severe convective storms. However, this approximation, when applied to the New Jersey data, results in a standard deviation for Z(p) of less than 1.6 dB and appears to be more representative than is $Z = 200\ R^{1.6}$ for the actual relationship between Z(p) and R(p) for convective storms.

9.0 THE EFFECT OF RAINFALL INTEGRATION INTERVAL UPON THE PROBABILITY DISTRIBUTION FUNCTION.

Because the relationship $Z(p) = 127.7\ R(p)^{2.26}$ was derived by considering 15-minute rainfall accumulations rather than the hourly accumulations normally available in most areas, there arises a problem in connection with the application of that relationship or any such relationship in a practical allocations plan. (47, 48, 49, 59)

There appears to be an additional requirement for

(1) A statistical link between the probability distribution functions for various integration periods, or

(2) A showing that the difference in probability distribution functions is insignificant within the limits of the extrapolation of the data.

Basically, the determination of a rainfall rate from the accumulation for any given period amounts to obtaining the mean or average value of the instantaneous rainfall in a sample size corresponding to the length of the period. The distribution of rainfall rates computed in this manner is actually the sampling distribution of the means (or averages). Since the population is infinite for all practical purposes and the number of samples is large, the sampling distribution of the means must be approximately normal regardless of the size of the samples (length of the accumulation period) and the distribution of the population (instantaneous rainfall rates) itself.* Since one has almost no chance of determining the instantaneous rainfall rates either directly or by the manipulation of rainfall accumulations, and is almost certain to encounter difficulties in determining the distribution function for the high rainfall rates which occur in very short time intervals in temperate climates, one is forced to the alternative (2), above.

To evaluate the effect of sampling interval differences upon the rainfall distribution function, a cumulative probability distribution of the hourly accumulations of the U. S. W. B. rain gauges at Cape May, Freehold, Glassboro, Hightstown, Lumberton, Marlton, and NAFEC was generated for the same time periods covered by the probability distribution derived from the 15-minute accumulations. An adjustment of this distribution function at points of equal probability by a least squares fit of the regression line (8-1) for p(R) $1.0 \leq R \leq$ Max. mm/hr. resulted in the relationship:

$$Z(p) = 99.4\ R(p)^{2.55} \qquad (9\text{-}1)$$

---

* / Special case of central limit theorem of probability theory.

The application of the approximation developed from the 15-minute rain gauge data $Z(p) = 127.7\ R(p)^{2.26}$ to the distribution function of the hourly data increases the standard deviation for Z(p) from 1.57 to 2.38 dB for the New Jersey data. Based upon this criterion alone, one might be persuaded to use the approximation resulting from the least squares fit of the regression line of the hourly rain gauge data in spite of the fact that the distribution contains only one quarter the number of samples found in the distribution for the shorter time period and the maximum rainfall rate is reduced from over 100 mm/hr. to approximately 40 mm/hr. Manipulation of the time increments of the rainfall accumulations of the seven U. S. W. B. rain gauges used in the POPSI Project does not represent an unbiased test of either the relationship of (8-2) or that of (9-1). A more significant test was made by considering the probability distributions for the hourly precipitation accumulations obtained from the Local Climatological Data for the U. S. W. B. stations at Atlantic City, Philadelphia, Newark, and Trenton, during the period covered by the POPSI data. These precipitation data are in the form readily available in most areas. In Figure 19 the probability distributions of the hourly rain gauge accumulations are compared with those derived from the 15-minute accumulations. The least squares fit regression lines of log Z(p) upon log R(p) are shown in Figure 20 and summarized in Table II which indicates the "goodness of fit" of each relationship to the data from which it was derived. Table III summarizes the results of testing the various Z(p) - R(p) approximations on rain gauge data other than that from which each relationship was derived. Although the differences in the standard errors of estimate of each approximation are not really significant, the test on independent data indicates that the $Z(p) = 127.7\ R(p)^{2.26}$ approximation is the best within the limits of the extrapolation of the New Jersey data.

10. CONCLUSION

The detailed analyses of the POPSI Project precipitation data have resulted in a useable Z-R relationship based upon measurements of the scattered electromagnetic field. By using the relationship $Z(p) = 127.7\ R(p)^{2.26}$, in conjunction with the probability distribution of high surface rainfall rates, the probability of exceeding a critical effective radar reflectivity in a given common volume can be calculated.

The problems of the altitude variability of the effective reflectivities, discrete scattering volume definition and identification of the exact nature of the scatterers dictate against the extrapolation of low rainfall rate Z-R relationships to the high rates which are pertinent to the calculation of possible interference due to precipitation scattering.

11.0 ACKNOWLEDGEMENTS

Acknowledgement is made of significant contributions to this research effort by personnel of the U. S. Air Force, U. S. Coast Guard, U. S. Weather Bureau, Federal Aviation Administration, AVCO Corporation and the Federal Communications Commission Laboratory Division. Dr. Robert K. Crane of Lincoln Laboratory, MIT, and Arnold G. Skrivseth and Harry Fine of the FCC Research Division provided technical advice and encouragement. Eugene D. Harris reviewed the final drafts and Russel G. Wilkins assisted with the reproduction.

Daniel B. Hutton, who passed away in September of 1969 was a co-author of the first POPSI Report and also made a significant contribution to the research leading to this present report.

12.0 BIBLIOGRAPHY

1. Carey, R. B., Kalagian, G. S. and Hutton, D. B. — FCC-USAF PCPSI Project, FCC Research Division Report No. R-6801, March 15, 1968.

2. NASA/ITS — Radio-Frequency Interference and Propagation Program Plan, August 25, 1969.

3. Du Castel, F. — Tropospheric Radiowave Propagation Beyond the Horizon, Pergamon Press, 1966.

4. Bean, B. R. and Dutton, E. J. — Radio Meteorology, NBS Monograph 92, March 1, 1966.

5. Wexler, Raymond — Radar Echoes from a Growing Thunderstorm, Journal of Meteorology, Vol. 10, August 1953.

6. Battan, Louis J. — Observations on the Formation and Spread of Precipitation and Convective Clouds, Journal of Meteorology, Vol. 10, No. 5, October 1953.

7. Donaldson, Ralph J. — Analysis of Severe Convective Storms Observed by Radar, Journal of Meteorology, Vol. 15. February 1958.

8. Falcone, V. J. Jr., and Dyer, R. — Refraction, Attenuation and Backscattering of Electromagnetic Waves in the Troposphere: A Revision of Chapter 9, Handbook of Geophysics and Space Environments, Air Force Cambridge Research Laboratories, January 1970.

9. Cole, A. E. et al — Precipitation and Clouds: Revision of Chapter 5, Handbook of Geophysics and Space Environments, November 1969.

10. Nathanson, F. E. and Reilly, J. P. — Radar Precipitation Echoes, IEEE Transactions Aerospace and Electronic Systems, Vol. AES-4, No. 4, July 1968.

11. Chi-Chen, Lee — The Meteorological Radar Equation for the Coherent Scattering of Radar Waves By Cloud Droplets and Raindrops, Research Translation, AFCRL, Acta Meteorological Sinica, Peking, China 32(2): 119-128, June 1962.

12. Culnan, D. E., Guiraud, F. O. — Radio Scattering Cross Sections of Thunderstorms, NBS Report 8816, June 9, 1965.

13. Crane, R. K. — Microwave Scattering Parameters for New England Rain, Technical Report 426, 3 October 1966, Lincoln Lab., MIT.

14. Crane, R. K. — Simultaneous Radar and Radiometer Measurements of Rain Shower Structure, Technical Note 1968-33, 18 September 1968, Lincoln Lab., MIT.

15. Doherty, L. H. and Stone, S. A. — Forward Scatter from Rain, PGAP Transactions, July, 1960.

16. Gunn, K. L. S. and East, T. R. W. — The Microwave Properties of Precipitation Particles, J. Royal Meteorological Soc., Vol. 80, pp. 522-545, 1954.

17. Usikov, A. Ya. et. al — Investigation of Absorption and Scattering of Millimeter Waves in Precipitations, I, II, Ukrainskii Fizichnii Zhrunal, Vol. 6, No. 5 pp. 618-641, 1961.

18. Blanchard, Duncan C. — Raindrop Size Distribution in Hawaiian Rains, J. of Meteorology, Vol. 10, December 1953.

19. Atlas, David and Plank, V. G. — Drop-Size History During a Shower, J. of Meteorology, Vol. 10, August 1953.

20. Spilhaus, Athelstan F. — Drop Size, Intensity and Radar Echo of Rain, J. of Meteorology, Vol. 5, August 1948.

21. Marshall, J. S. and Palmer, W. McK. — The Distribution of Raindrops with Size, J. of Meteorology, Vol. 5, August 1948.

22. Wexler, Raymond — Rain Intensities by Radar, J. of Meteorology, Vol. 5, August 1948.

23. Marshall, J. S. et al — Measurement of Rainfall by Radar, J. of Meteorology, Vol. 4, 186-192.

24. Laws, J. O. and Parsons, D. A. — The Relation of Raindrop-Size to Intensity, Trans. Amer. Geophysical Union Vol. 24, Part II, 452-459 (1943).

25. Altman, F. J. — Precipitation Scatter Interference Between Space and Terrestrial Communications Systems, CSI Report No. 453340, October, 1967.

26. Kell, R. E. — On the Derivation of Bistatic RCS from Monostatic Measurements, Proc. of the IEEE, Vol. 53, No. 8 August, 1965.

27. Herman, B. M. and Battan, L. J. — Calculations of Mie Back-Scattering of Microwaves from Ice Spheres, Quart, J. Royal, Meteorol. Soc. 87, 223-230, 1961 a.

28. Wheeler, Albert D. — Radio-wave Scattering by Tropospheric Irregularties, J. of Research of NBS, Vol. 2, September-October 1959.

29. Bowker, A H. and Lieberman, G. J. — Engineering Statistics, Prentice-Hall Inc. Englewood Cliffs, N. J. 1959.

30. Lefkowitz, Matthew and McCann, Robert J. — Review of the Atlantic City MESONET, Final Report, SRDS Report No. RD-69-20, U. S. Dept. of Comm., ESSA, Weather Bureau, Sterling, Va. March, 1969.

31. Ross, Martin — Radar-Computed Rainfall Compared with Observations from a Dense Network of Rain Gauges, USAF ETAC TN 69-4, June 1969.

32. Kostarev, V. V. and Chernickov, A. A. — Increasing the Accuracy of Radar Measurement of Precipitation, Meteorologiia i Hydrologiia No. 7, pp. 102-106, 1969.

33. Divinskaia, B. Sh. — Radar Analysis of Cloud and Precipitation Fields, Leningrad. Glavnaia Geofizicheskaia, Trudy No. 173: 34-52, 1965.

34. Jones, D. M. A. — Final Report, Program in Atmospheric Electricity and Cloud Modification Flagstaff-1966, Technical Report ECOM-02376-F, June 15, 1967.

35. Wilson, James W. — Evaulation of Precipitation Measurements with the WSR-57 Weather Radar, Jour. of Applied Meteorology, Vol. 3., 164-174, April, 1964.

36. Hogg, D. C. — Statistics on Attenuation of Microwaves by Intense Rain, Bell System Technical Journal, Vol. 48, No. 9, November, 1969.

37. Saliman, E. M. and Zhupakhin, K. S. — Some Results of Radar Investigations of the Vertical Structures of Showers and Thunderstorms, Research Translation, AFCRL, Leningrad, Glavnia Geofizicheskaia Observatoriia, Trudy, No. 159, 59-64, 1964.

38. Hanks, Howard H. Jr. and Long, Michael J. — The Rate of Growth of Tall Thunderstorms, Final Report, AFCRL - 69-0388 Sept., 1969.

39. Mitchell, R. L. — Remote Sensing of Rain by Radar, Aerospace Report No. TR-0158(3525-09) -1, January 1968.

40. Battan, Louis J. and Herman, Benjamin M. — The Radar Cross Sections of "Spongy" Ice Spheres., J. of Geophysical Research, Vol. 67, No. 13. December 1962.

41. Atlas, David et al — Radar Reflectivity of Storms Containing Spongy Hail, J. of Geophysical Research, Vol. 69, No. 10, May 15, 1964.

42. Modahl, A. F. — The Influence of Vertical Wind Shear on Hailstorm Development and Structure, Dept. of Atmospheric Science, Colo. State University Paper No. 137, March 1969.

43. Srivastave, P. C. et al — Growth, Motion and Concentration of Precipitation Particles in Convective Storms. Chicago Univ. Ill. Dept. of Geophysical Sciences NSF GA 919, 18 Nov. 1968.

44. Fischer, R. E. — Remote Sensing of Hail and Hail Growth in Convective Clouds, Dept. of Atmospheric Science, Colo. State Univ. Paper No. 141, June 1969.

45. Hamilton, R. E. — A Review of Use of Radar in Detection of Tornadoes and Hail, Weather Bureau, Garden City, N. J. Eastern Regional Hqtrs. WBTM ER 34, December, 1969.

46. Mueller, E. A. and Sims, A. L. — Relationships Between Reflectivity, Attenuation and Rainfall Rate Derived from Drop Size Spectrum. Rand Report ECOM-02071-F U. S. Army Electronics Command April 1969.

47. Bussey, H. E. — Microwave Attentuation Statistics Estimated From Rainfall and Water Vapor Statistics, Pro. of the IRE Vol. 38, No. 7, July 1950.

48. Burroughs, H. H. — Rain Intensity Time Distributions, Naval Ordnance Lab. Corona, Calif. NOLC Report 729, 15 June 1967.

49. Russak, S. L. and Easley, J. W. — A Practical Method for Estimating Rainfall Rate Frequencies Directly from Climatic Data, Bulletin of the American Meteorological Society Vol. 39, No. 9, Sept. 1958, pp 469-472.

50. Carey, R. B. and Kalagian, G. S. — Detailed Analysis of FCC/USAF POPSI Project Data, URSI 1969 Fall Meeting, Austin, Texas.

51. Deam, A. P. Fowler, M. S. and La Grone, A. H. — Bistatic Radar Observations of Drop Size Distribution in a Rain Shower, Univ. of Texas Report No. P-17, 17 Nov. 1967.

52. Deam, A. P. Fowler, M. S. and La Grone, A. H. — Comparison of Bistatic and Monostatic Radar Observations with Rain Rate Measurements on the Ground, Antennas and Propagation Division, Electrical Engineering Research Lab. Univ. of Texas at Austin, Report No. P-16, 23 January 1968.

53. Crane, R. K. — A Comparison Between Monostatic and Bistatic Scattering from Rain and Thin Turbulent Layers, MIT Lincoln Lab. Tech. Note 1970-29, 6 October 1970.

54. Gjessing, Dag T — Scattering of Radio Waves from Regular and Irregular Time Varying Refractive Index Structures in the Troposphere, Norwegian Defence Research Establishment Report, Kjeller, Norway, 1968.

55. Wexler, Raymond and Atlas, David — Moisture Supply and Growth of Stratiform Precipitation, J. of Meteorology, Vol. 15, December 1958.

56. Austin, P. M. and Bemis, A. C. — A Quantitative Study of the Bright Band in Radar Precipitation Echoes, J. of Meteorology, Vol. 7, 145-151, (1950).

57. Huff, F. H. and Changnon, S. A. Jr. — Development and Utilization of Illinois Precipitation Networks, Illinois State Water Survey Reprint Series No. 56, 1966.

58. No author — Weather Surveillance Radar Manual, U. S. Dept. of Commerce, 1962.

59. Gusler, L. T. and Hogg, D. C. — Some Calculations on Coupling Between Satellite Communications and Terrestrial Radio-Relay Systems Due to Scattering by Rain, B. S. T. J. Vol. 49, No. 7, Sept. 1970.

TABLE I

Common Volume Groups

Site	TX Ant. Az.	TX Ant. Elev.	RX Ant. Az.	Alt. of CV	Period	Group
WW	3	1/2	3	0.7-2.1 Km	2/16-5/13	I
"	6	1/2	3	0.7-1.4	" "	I
"	6	1	3	1.0-2.2	" "	I
"	6	1/2	6	0.8-2.0	5/14-6/7	A
NAF	3	1/2	6	0.7-1.6	" "	A
"	3	1	6	1.202.1	" "	A
"	6	1/2	6	1.0-1.3	" "	A
"	6	1	6	1.1-1.9	" "	A
"	12	2	6	1.6-2.0	6/7-8/16	A
WW	3	1	3	1.2-3.0	2/16-5/13	II
"	6	2	3	1.6-3.4	" "	II
"	6	1	6	1.4-2.9	5/14-6/7	B
"	3	1/2	6	1.0-2.4	" "	B
"	3	1	6	1.9-2.9	" "	B
NAF	3	2	6	2.3-2.6	" "	B
"	6	2	6	1.7-2.9	" "	B
"	9	2	6	1.6-2.4	6/7-8/16	B
"	12	3	6	1.9-2.8	" "	B
"	12	4	3	2.0-2.4	8/19-10/24	V
"	12	6	3	2.2-3.6	" "	V
"	18	8	3	2.3-3.4	" "	V
WW	3	2	3	2.1-3.8	2/16-5/13	III
"	3	3	3	3.0-4.3	" "	III
"	6	3	3	2.1-4.3	" "	III
"	6	4	3	2.8-4.9	" "	III
"	6	2	6	2.6-3.8	5/14-6/7	C
"	9	2	6	2.4-3.6	6/7-8/16	C
"	12	3	6	2.8-4.3	" "	D
NAF	6	3	6	2.5-3.4	5/14-6/7	C
"	9	3	6	2.1-3.3	6/7-8/16	C
"	9	4	6	2.7-3.8	" "	C
"	12	4	6	2.4-3.5	" "	C
"	9	5	6	3.4-4.1	" "	D
"	12	5	6	2.9-4.1	" "	D
"	12	6	6	3.4-4.4	" "	D
"	12	7	6	4.1-4.5	" "	D
"	12	8	3	2.5-4.5	8/19-10/24	W
"	18	10	3	2.5-4.2	" "	W
"	18	12	3	2.8-4.8	" "	W

TABLE I
(2)

Common Volume Groups

Site	TX Ant. Az.	TX Ant. Elev.	RX Ant. Az.	Alt. of CV	Period	Group
WW	6	5	3	3.4-5.3	2/16-5/13	IV
"	6	6	3	4.2-5.4	" "	IV
"	9	3	6	3.2-5.1	6/7-8/16	E
"	12	4	6	3.6-5.6	" "	E
"	12	6	3	3.5-5.4	8/19-10/24	X
"	18	8	3	3.0-4.9	" "	X
"	18	10	3	4.1-5.1	8/19-10/24	X
NAF	12	10	3	3.0-5.1	" "	X
"	12	12	3	3.4-5.3	" "	X
"	12	14	3	3.9-5.4	" "	X
"	12	16	3	4.5-5.5	" "	X
"	18	14	3	3.1-5.3	" "	X
"	18	16	3	3.4-5.6	" "	X
WW	9	4	6	4.2-6.1	6/7-8/16	F
"	9	5	6	5.1-6.6	" "	F
"	12	5	6	4.3-6.4	" "	F
"	12	6	6	5.2-7.0	" "	F
"	12	7	6	6.1-7.4	" "	F
"	12	8	3	4.2-6.9	8/19-10/24	Y
"	12	10	3	4.7-7.9	" "	Y
"	18	12	3	4.5-7.4	" "	Y
"	18	14	3	5.0-8.2	" "	Y
"	12	12	3	5.4-8.4	" "	Z
"	12	14	3	6.1-8.7	" "	Z
"	12	16	3	6.8-8.8	" "	Z
"	18	16	3	5.4-8.8	" "	Z
"	18	18	3	5.9-9.2	" "	Z
"	18	20	3	6.4-9.4	" "	Z
NAF	18	18	3	3.7-5.8	" "	Y
"	18	20	3	4.1-5.9	" "	Y

Total number of common volume samples: 15,160

Number of active samples : 2214
(Signal adequate for determination of a median effective reflectivity)

Number of samples discarded due to indications of mixed mode or guided propagation. : 1241

Highest precipitation Z(eff.) : 2.13×10^6 mm^6 m^{-3}

Highest discarded Z(eff.) : 1.01×10^7 mm^6 m^{-3}

TABLE II

Goodness of Fit of Regression Lines

Least squares fit of regression line log Z(p) upon log R(p)	Source of Data for p(R)	Rainfall Accumulation Period	Maximum Rainfall Rate (mm/hr.)	Standard Error of Estimate of Z(p) from R(p)
$Z(p) = 127.7\ R(p)^{2.26}$	7 U.S.W.B. Rain Gauges of POPSI	15 minutes	105	1.57 dB
$Z(p) = 99.4\ R(p)^{2.55}$	Same	1 hour	39	2.08 dB
$Z(p) = 190.7\ R(p)^{1.85}$	Atlantic City	1 hour	57	1.33 dB
$Z(p) = 150.8\ R(p)^{2.15}$	Newark, N. J.	1 hour	30	1.37 dB
$Z(p) = 108.1\ R(p)^{2.21}$	Philadelphia, Penn.	1 hour	37	2.00 dB
$Z(p) = 97.1\ R(p)^{2.40}$	Trenton, N. J.	1 hour	24	2.16 dB
$Z(p) = 113.9\ R(p)^{2.31}$	Aggregate of Atlantic City, Newark, Philadelphia and Trenton.	1 hour	57	1.46 dB

TABLE III

Summary of Test of Z-R Relationships

Relationship	Source of p(R)	Rainfall Accumulation Period	Standard Deviation of Z(p) from POPSI data
$Z = 200\ R^{1.6}$	7 U.S.W.B. rain gagues of POPSI	15 minutes	6.52 dB
	Aggregrate of Atlantic City, Newark, Philadelphia and Trenton.	1 hour	6.17 dB
$Z(p) = 127.7\ R(p)^{2.26}$	7 U.S.W.B. rain gauges of POPSI.	1 hour	2.88 dB
	Atlantic City	1 hour	3.26 dB
	Newark, N. J.	1 hour	1.47 dB
	Philadelphia, Penn.	1 hour	2.32 dB
	Trenton, N. J.	1 hour	2.22 dB
	Aggregate of Atlantic City, Newark, Philadelphia and Trenton.	1 hour	1.48 dB
$Z(p) = 99.4\ R(p)^{2.55}$	Atlantic City	1 hour	5.42 dB
	Newark, N. J.	1 hour	2.79 dB
	Philadelphia, Penn.	1 hour	3.50 dB
	Trenton, N. J	1 hour	2.63 dB
	Aggregate of Atlantic City, Newark, Philadelphia and Trenton.	1 hour	2.67 dB

POPSI PROJECT
Meteorological Facilities

CV No.	RX Site	RX AZ	TX AZ
1	WW	3	3
2	WW	3	6
3	NAF	6	3
4	NAF	6	6
5	WW	6	3
6	WW	6	6
7	WW	6	9
8	WW	6	12
9	NAF	6	9
10	NAF	6	12
11	NAF	3	12
12	NAF	3	18
13	WW	3	12
14	WW	3	18

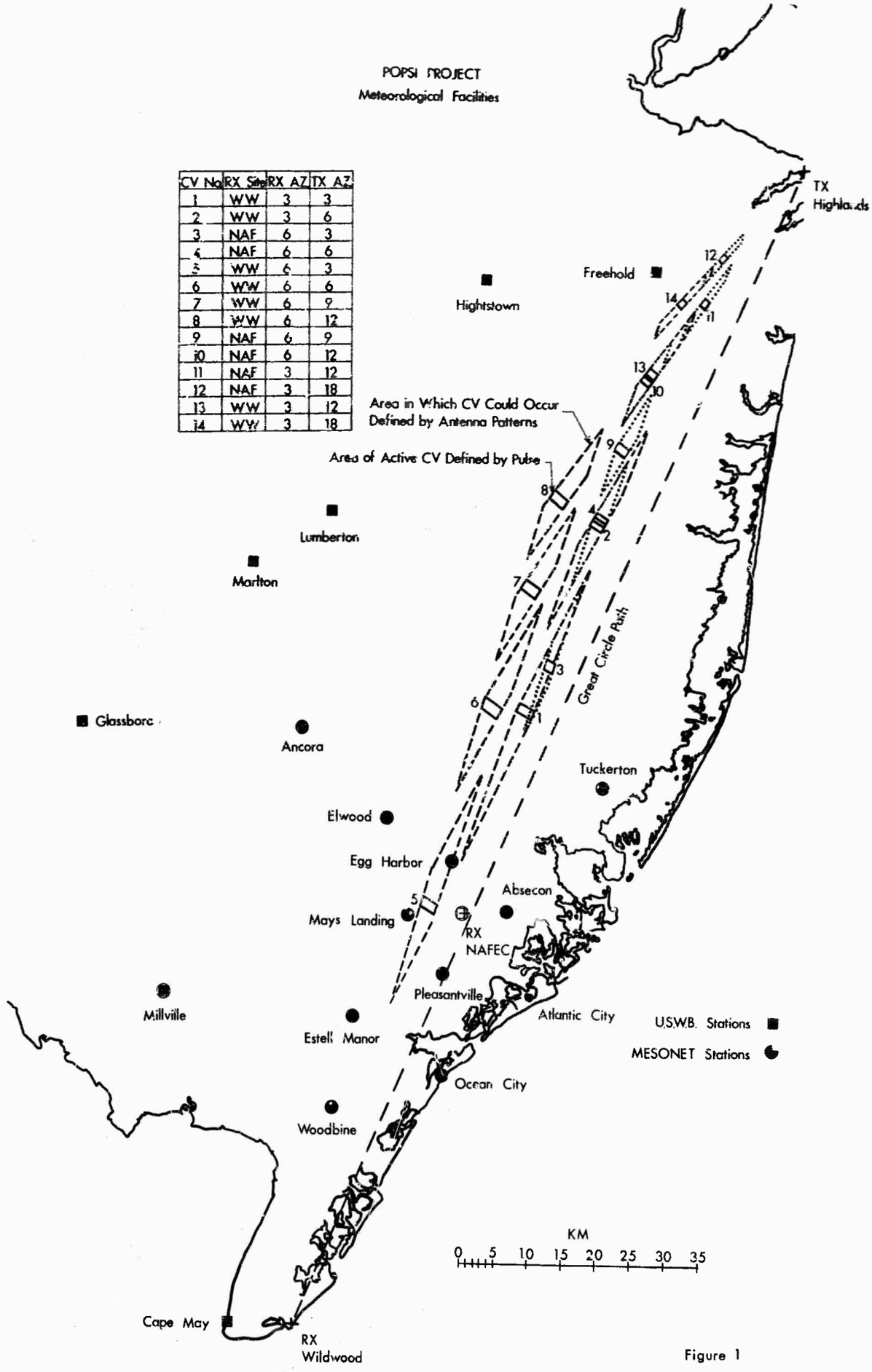

Figure 1

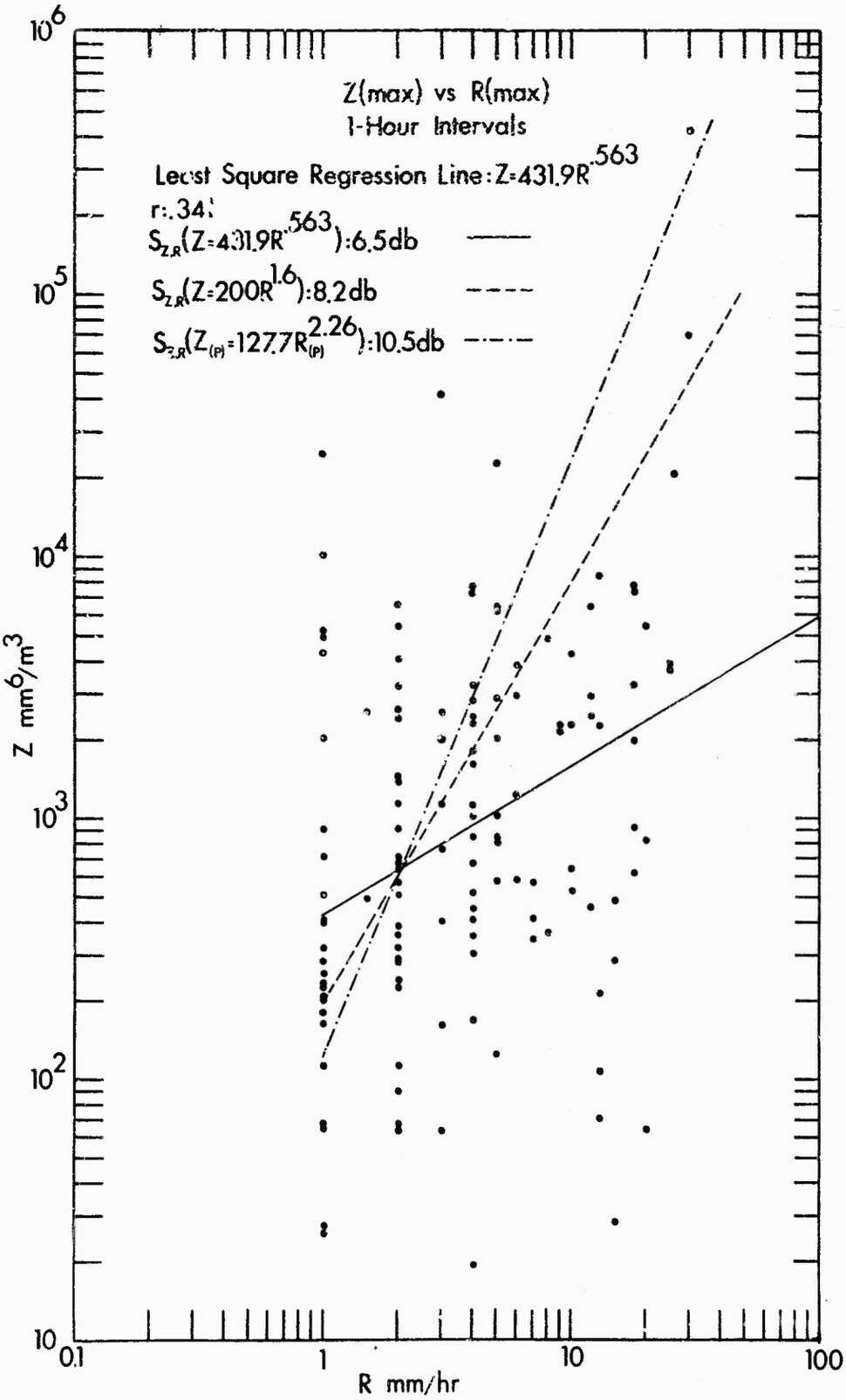
Z(max) vs R(max)
1-Hour Intervals
Least Square Regression Line: Z=431.9R^.563
r=.34
S_Z,R(Z=431.9R^.563):6.5db
S_Z,R(Z=200R^1.6):8.2db
S_Z,R(Z_(P)=127.7R_(P)^2.26):10.5db
Z mm^6/m^3
R mm/hr
10^6
10^5
10^4
10^3
10^2
10
0.1
1
10
100

Figure 2

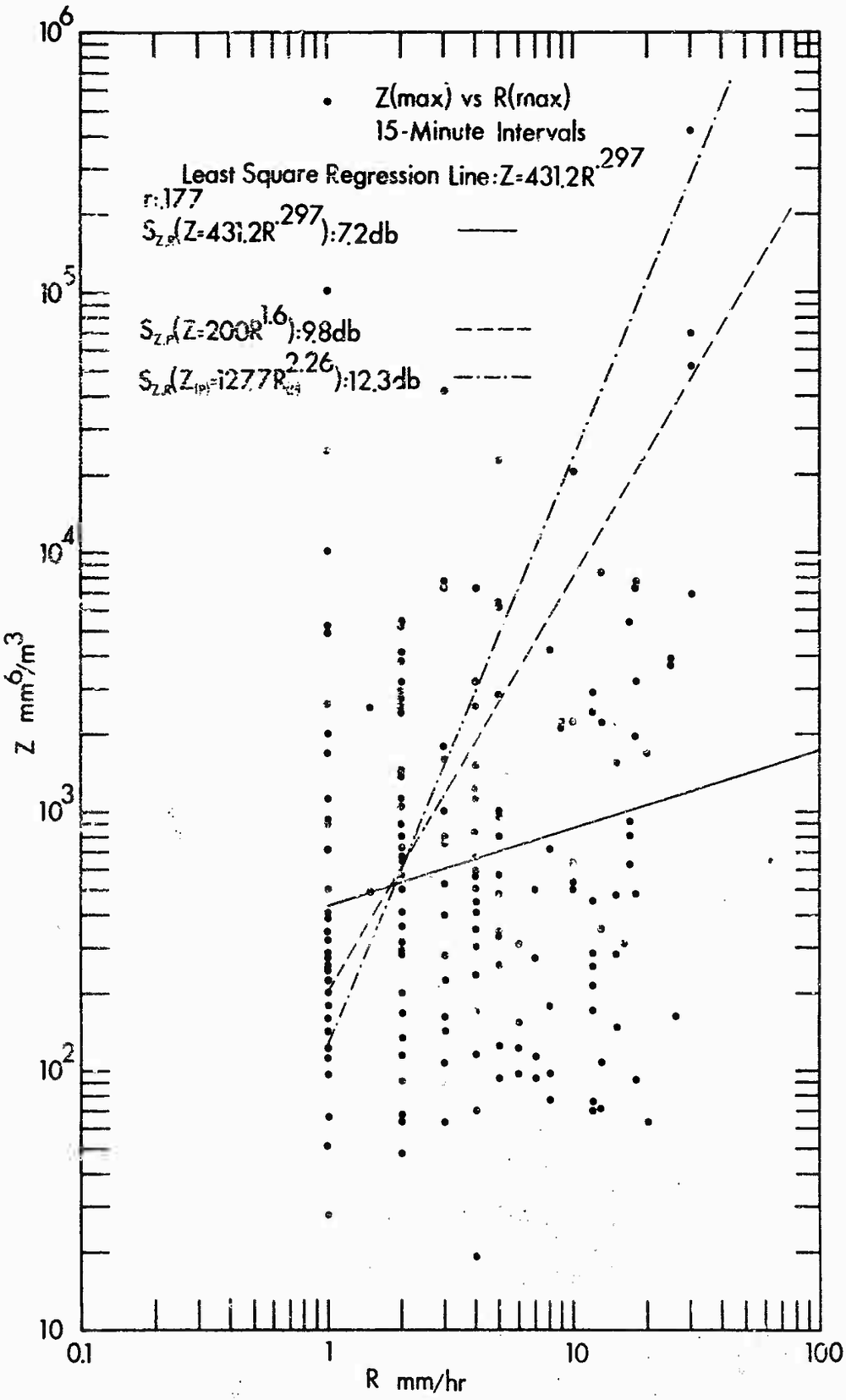
Z(max) vs R(max)
15-Minute Intervals
Least Square Regression Line: Z=431.2R^.297
r:.177
S_Z,R(Z=431.2R^.297):7.2db
S_Z,R(Z=200R^1.6):9.8db
S_Z,R(Z_(p)=1277R_(p)^2.26):12.3db
Z mm^6/m^3
R mm/hr
10^6
10^5
10^4
10^3
10^2
10
0.1
1
10
100

Figure 3

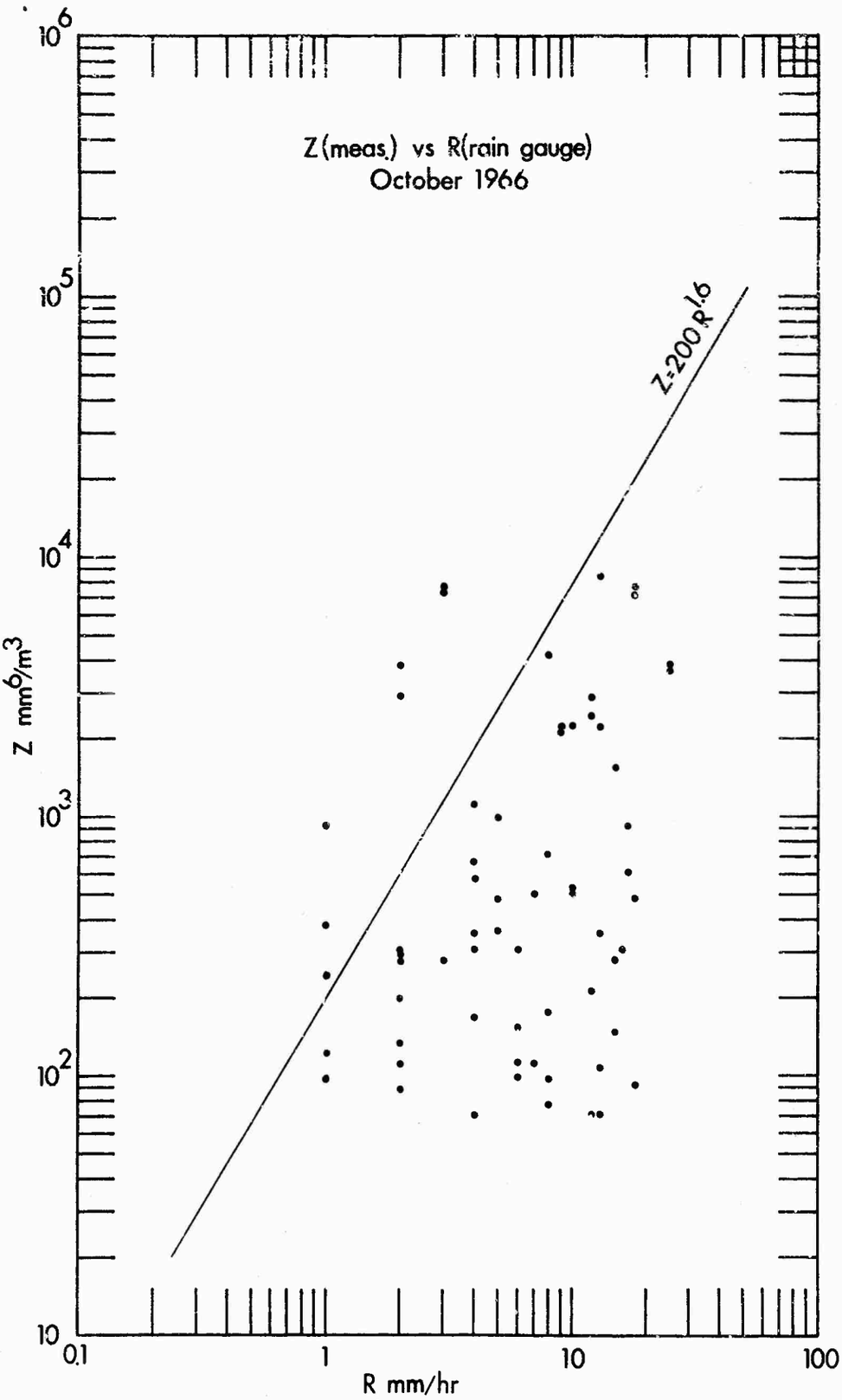
Z(meas.) vs R(rain gauge)
October 1966
Z=200.R^1.6
Z mm^6/m^3
R mm/hr
10^6
10^5
10^4
10^3
10^2
10
0.1
1
10
100

Figure 4

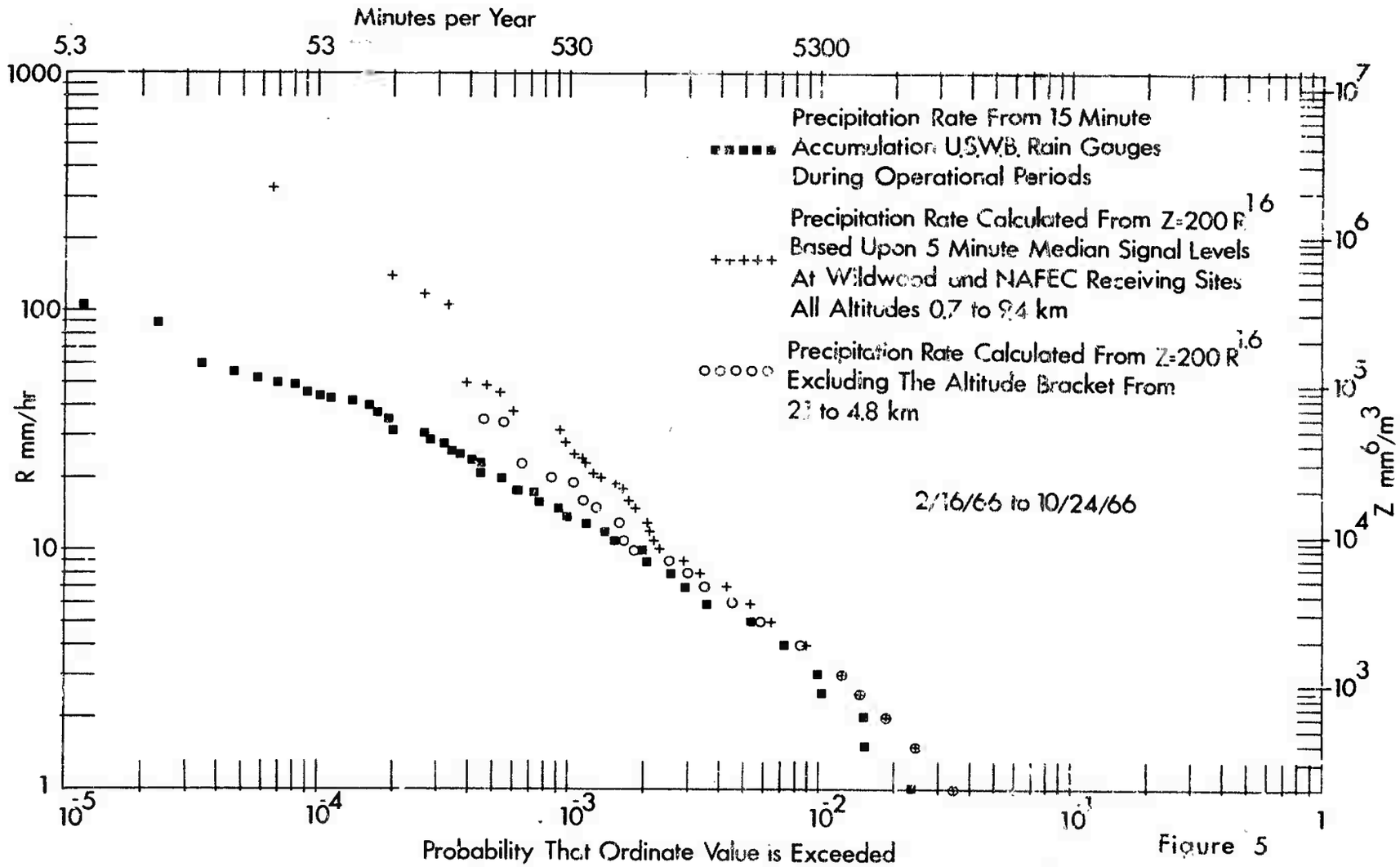
Minutes per Year
5.3
53
530
5300
1000
100
10
1
R mm/hr
10^7
10^6
10^5
10^4
10^3
Z mm^6/m^3
Precipitation Rate From 15 Minute Accumulation U.S.W.B. Rain Gauges During Operational Periods
Precipitation Rate Calculated From $Z=200R^{1.6}$ Based Upon 5 Minute Median Signal Levels At Wildwood and NAFEC Receiving Sites All Altitudes 0.7 to 9.4 km
Precipitation Rate Calculated From $Z=200R^{1.6}$ Excluding The Altitude Bracket From 2.3 to 4.8 km
2/16/66 to 10/24/66
10^{-5}
10^{-4}
10^{-3}
10^{-2}
10^{-1}
1
Probability That Ordinate Value is Exceeded

Figure 5

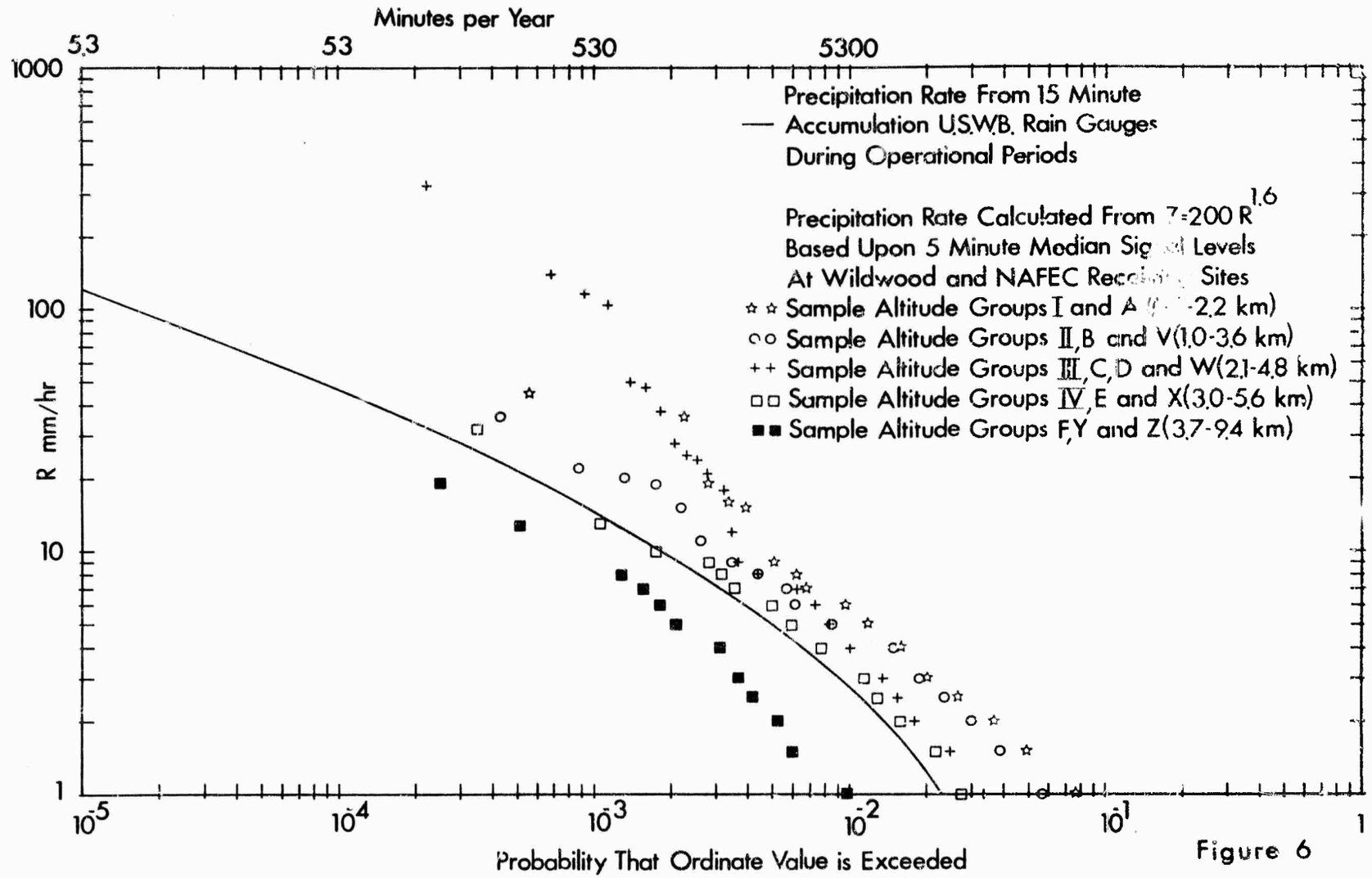
Minutes per Year
5.3
53
530
5300
1000
100
10
1
R mm/hr
Precipitation Rate From 15 Minute
Accumulation U.S.W.B. Rain Gauges
During Operational Periods
Precipitation Rate Calculated From Z=200 R^1.6
Based Upon 5 Minute Median Sig al Levels
At Wildwood and NAFEC Rec Sites
Sample Altitude Groups I and A -2.2 km)
Sample Altitude Groups II, B and V(1.0-3.6 km)
Sample Altitude Groups III, C, D and W(2.1-4.8 km)
Sample Altitude Groups IV, E and X(3.0-5.6 km)
Sample Altitude Groups F, Y and Z(3.7-9.4 km)
10^-5
10^-4
10^-3
10^-2
10^-1
1
Probability That Ordinate Value is Exceeded

Figure 6

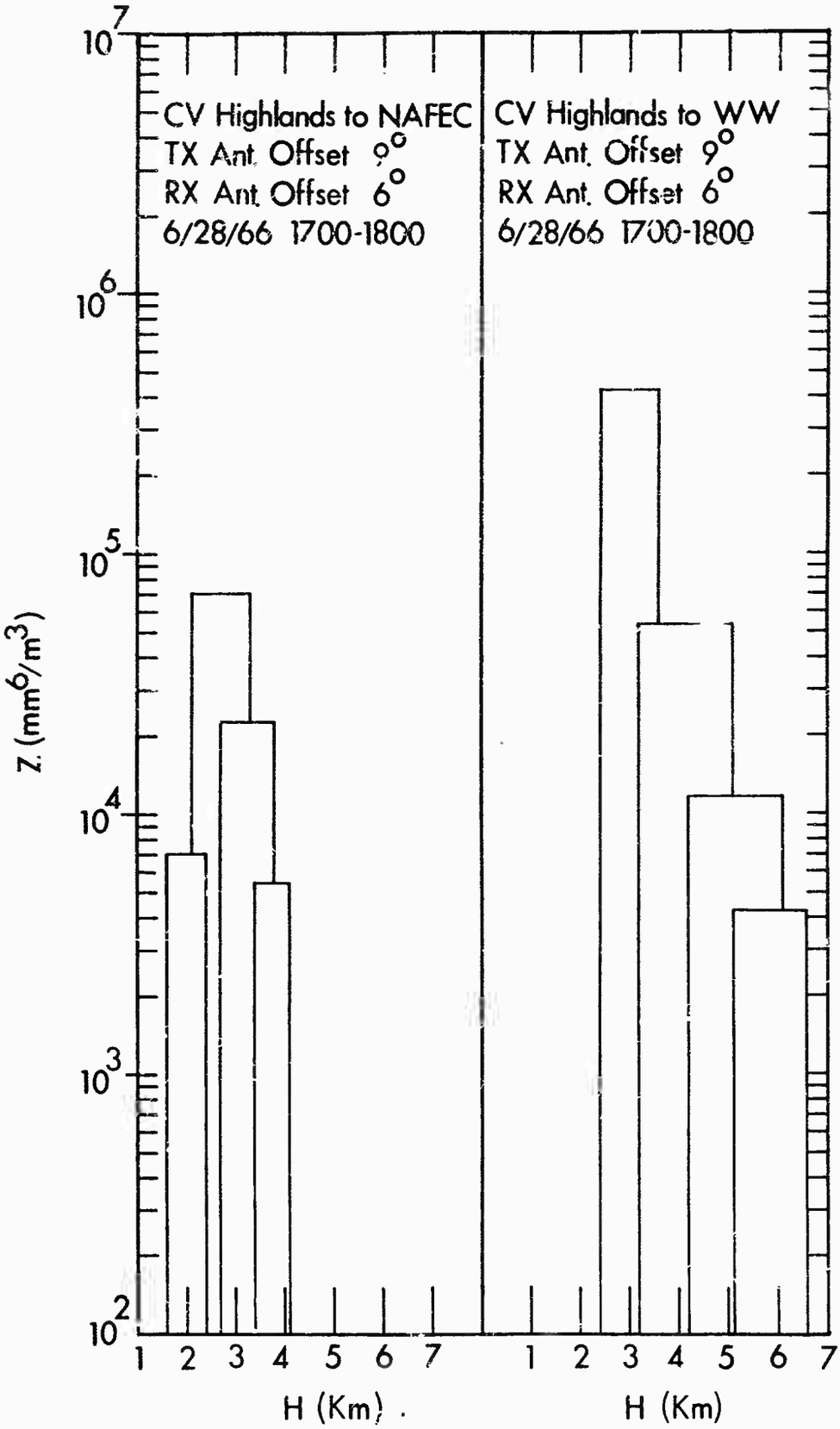
CV Highlands to NAFEC
TX Ant. Offset 9°
RX Ant. Offset 6°
6/28/66 1700-1800
CV Highlands to WW
TX Ant. Offset 9°
RX Ant. Offset 6°
6/28/66 1700-1800
Z (mm6/m3)
10^7
10^6
10^5
10^4
10^3
10^2
1 2 3 4 5 6 7
H (Km)
1 2 3 4 5 6 7
H (Km)

Figure 7

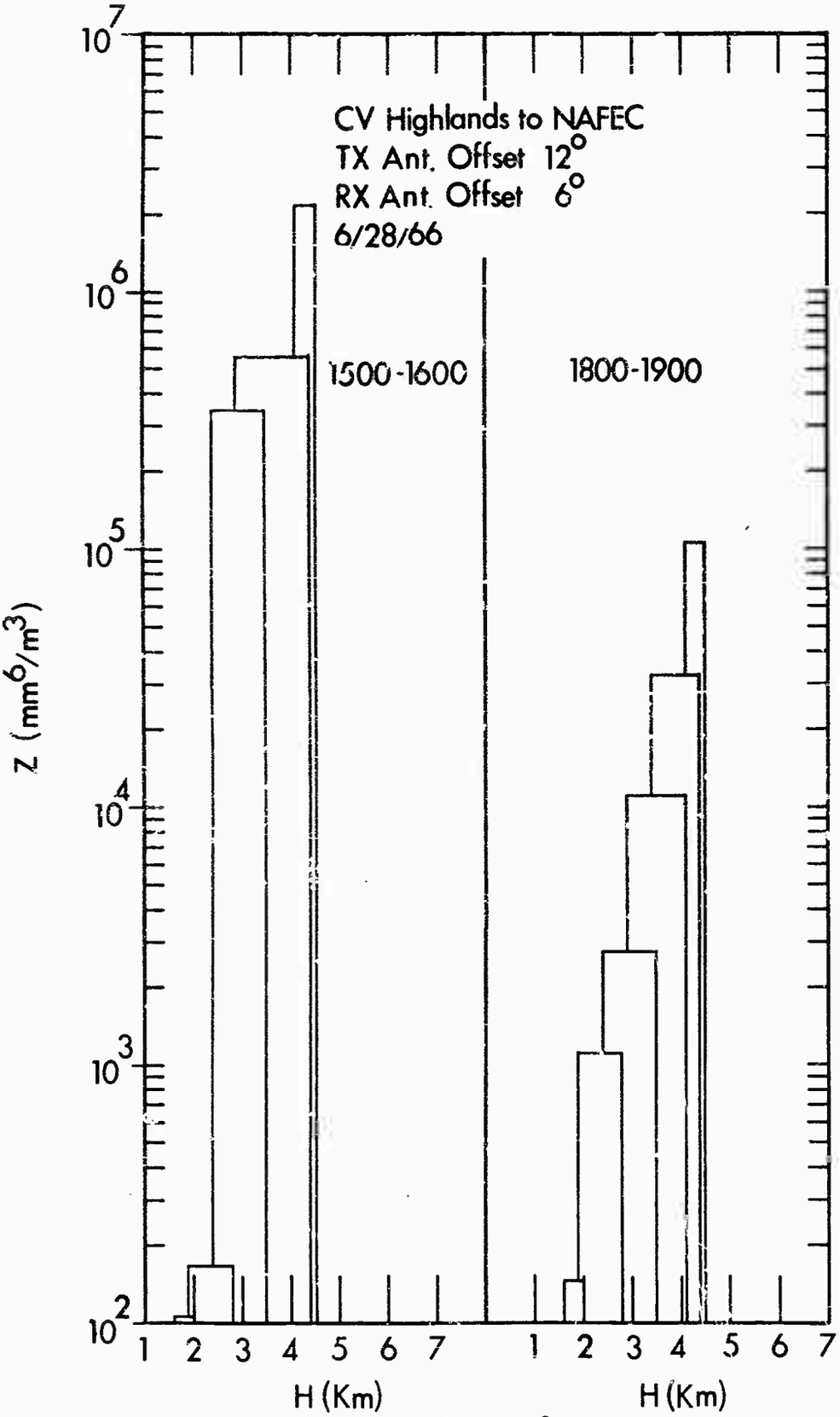
CV Highlands to NAFEC
TX Ant. Offset 12°
RX Ant. Offset 6°
6/28/66
1500-1600
1800-1900
Z (mm6/m3)
10^7
10^6
10^5
10^4
10^3
10^2
1 2 3 4 5 6 7
1 2 3 4 5 6 7
H (Km)
H (Km)

Figure 8

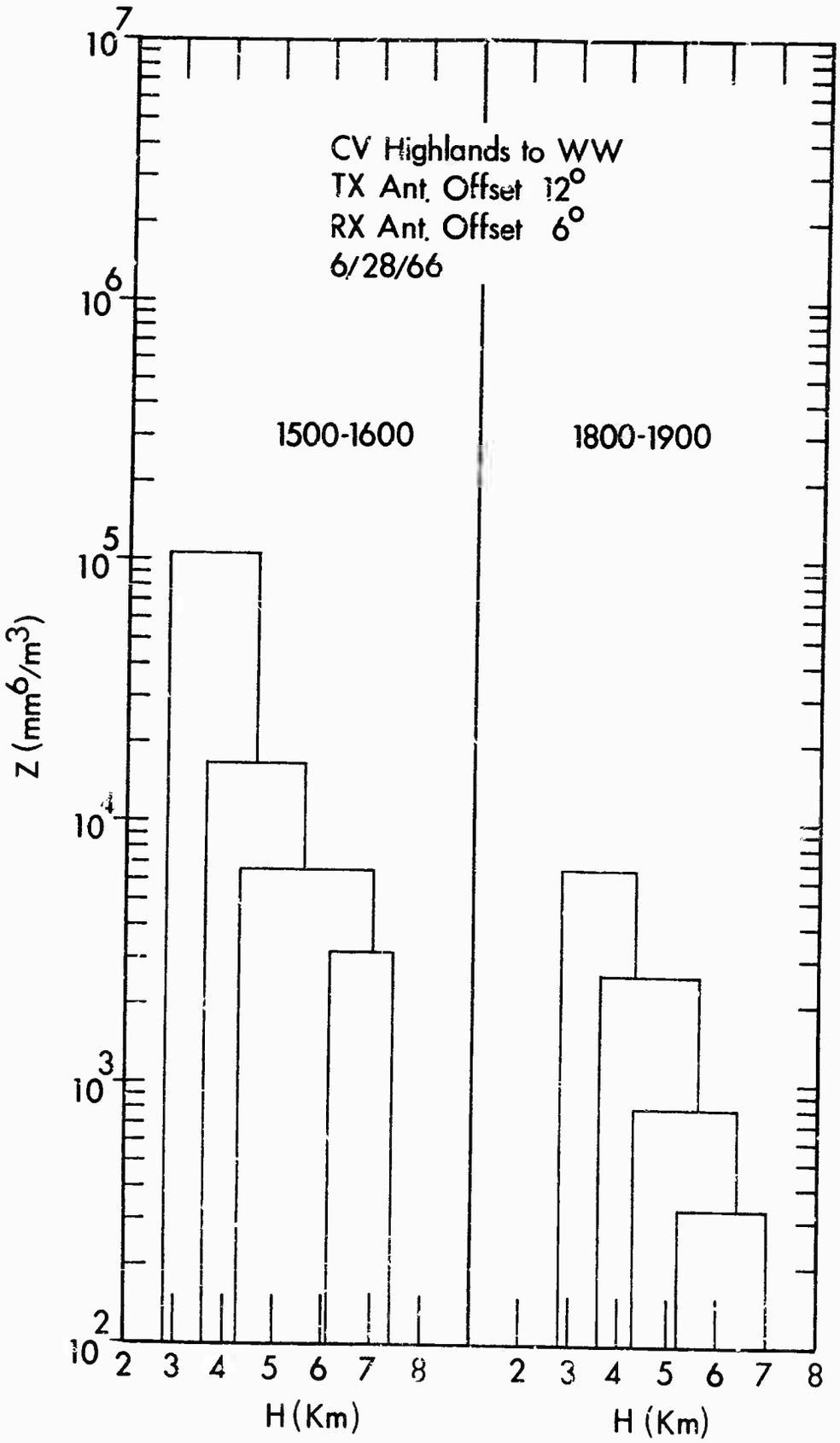
CV Highlands to WW
TX Ant. Offset 12°
RX Ant. Offset 6°
6/28/66
1500-1600
1800-1900
Z (mm6/m3)
10^7
10^6
10^5
10^4
10^3
10^2
2 3 4 5 6 7 8
2 3 4 5 6 7 8
H (Km)
H (Km)

Figure 9

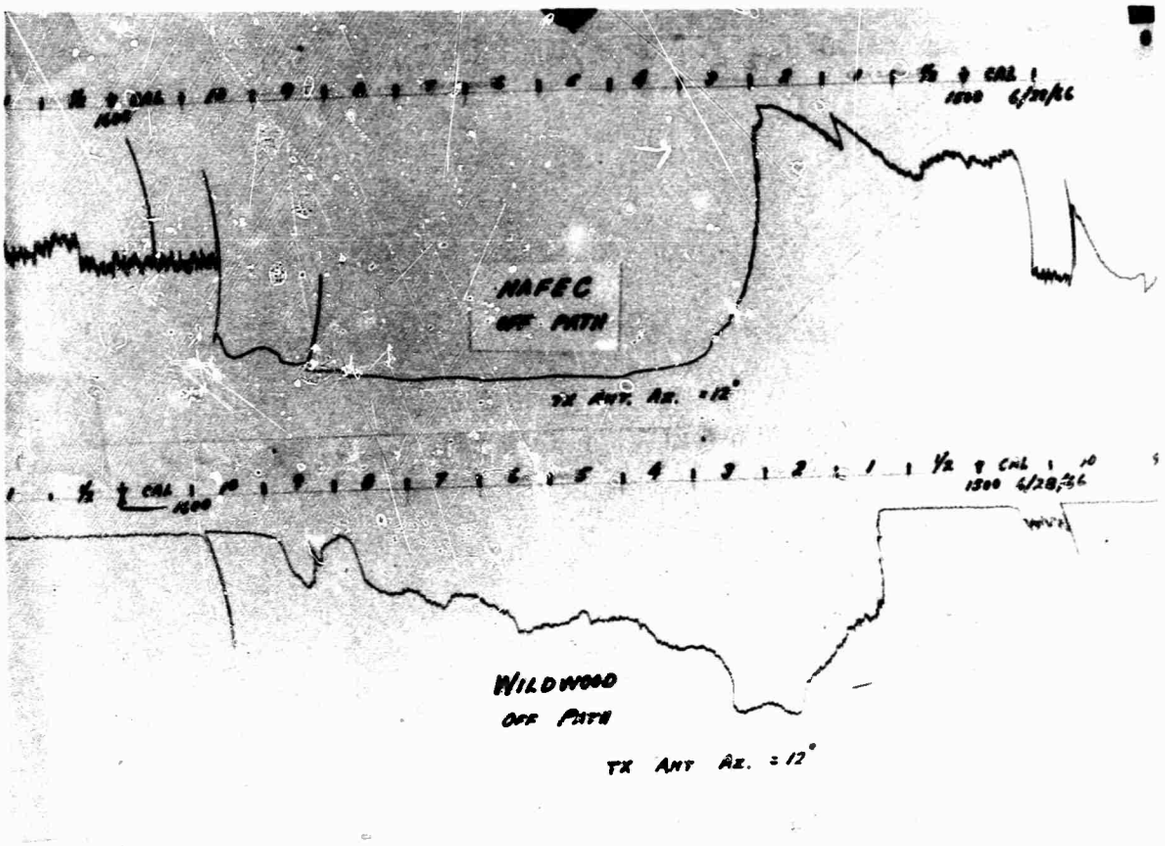

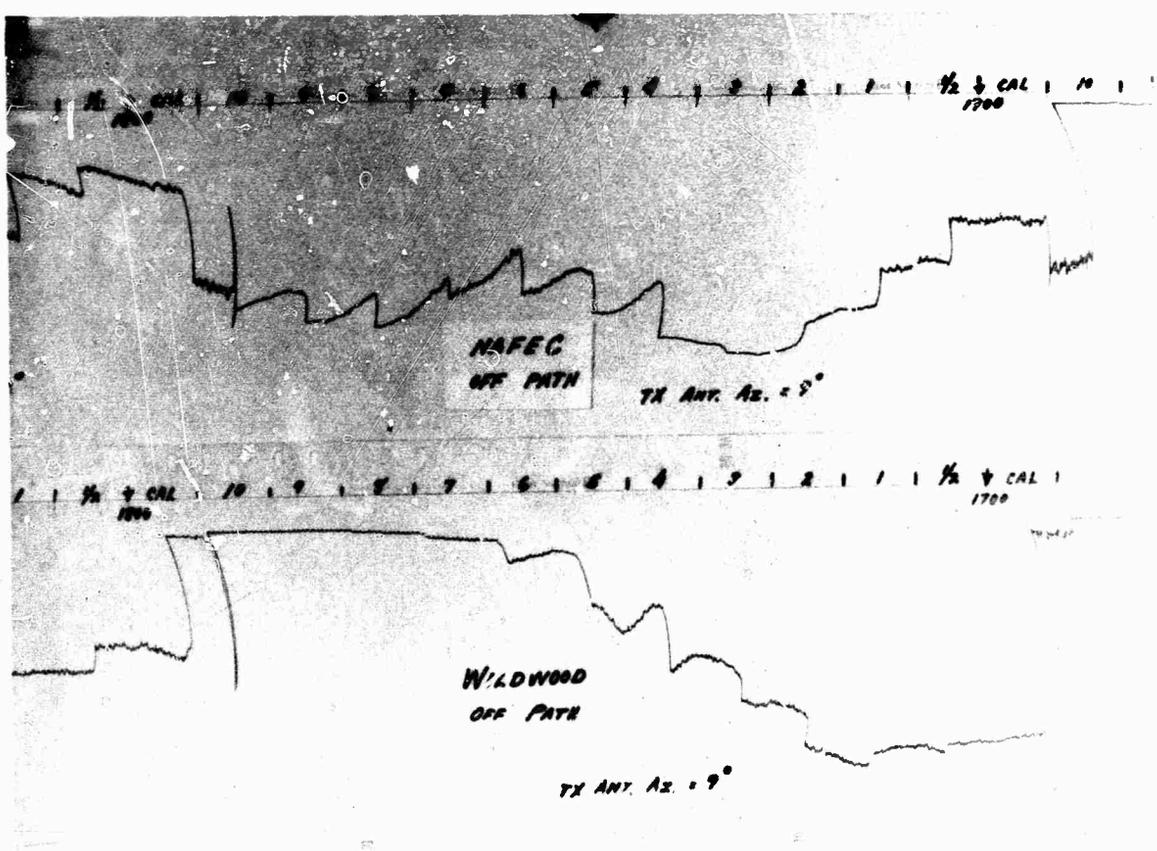

Recorder Charts Showing Fading Rate on 6-28
Figure 10

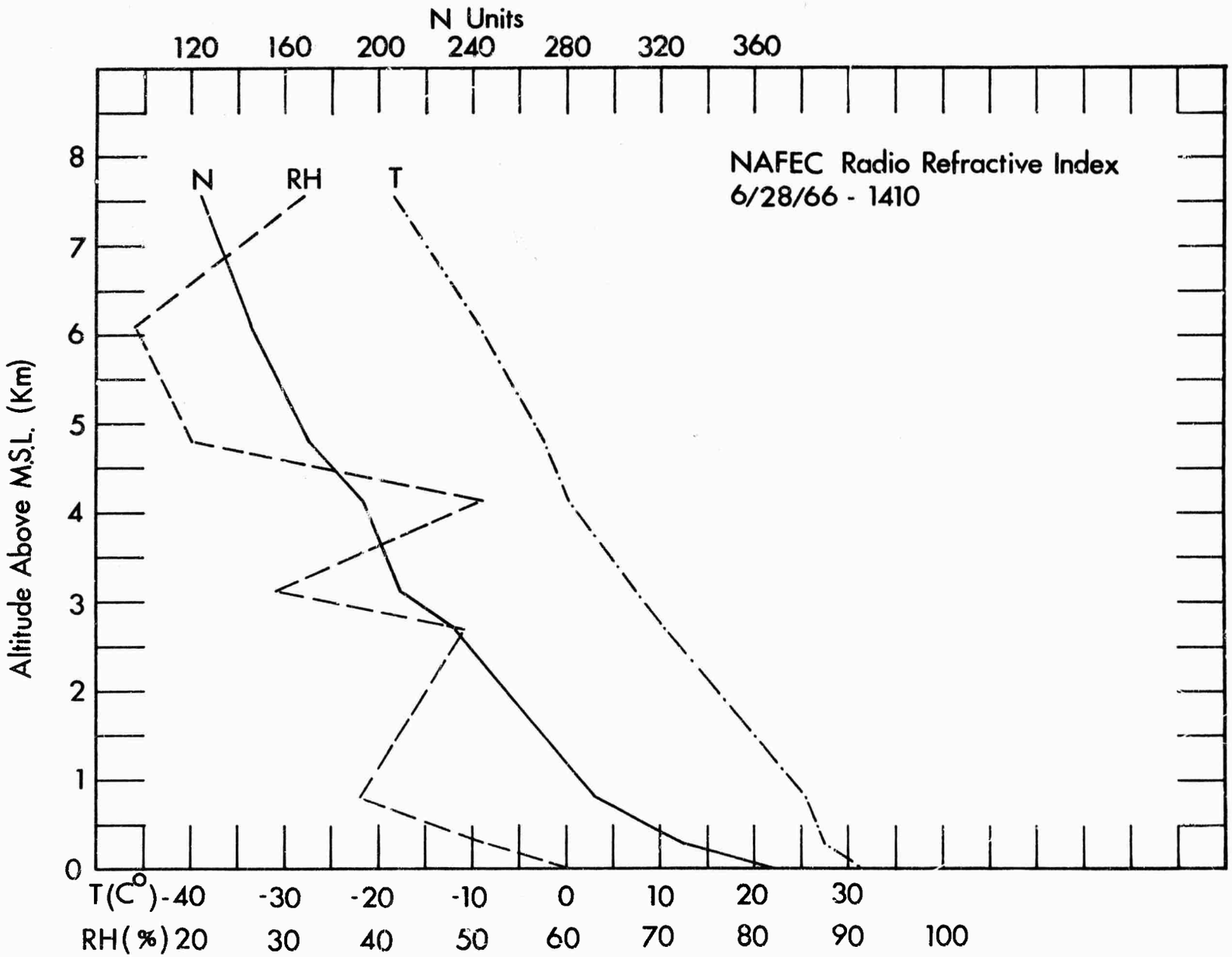
N Units
120 160 200 240 280 320 360
NAFEC Radio Refractive Index
6/28/66 - 1410
N
RH
T
Altitude Above M.S.L. (Km)
0 1 2 3 4 5 6 7 8
T(C°) -40 -30 -20 -10 0 10 20 30
RH(%) 20 30 40 50 60 70 80 90 100

Figure 11

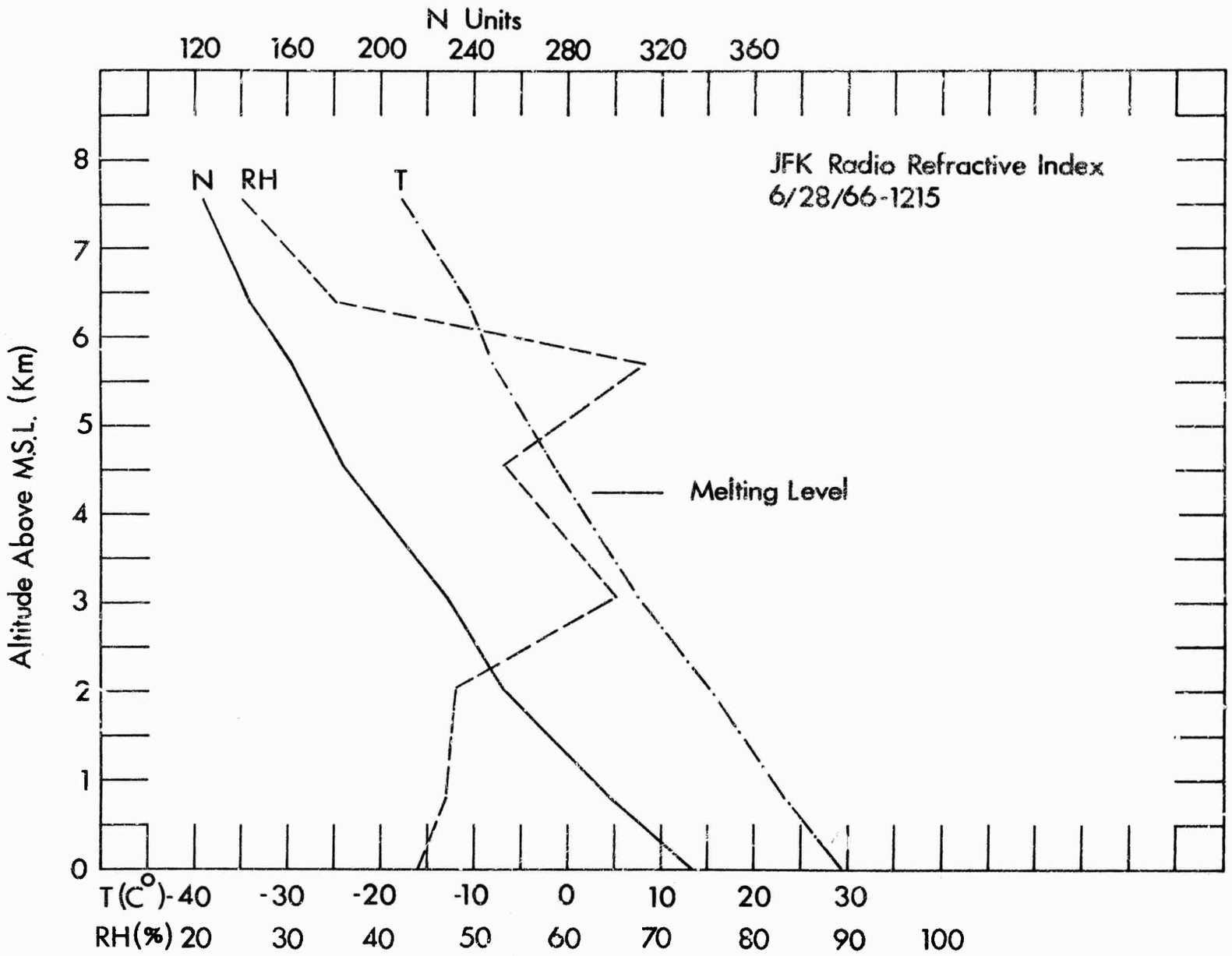
N Units
120
160
200
240
280
320
360
JFK Radio Refractive Index
6/28/66-1215
N
RH
T
Melting Level
Altitude Above M.S.L. (Km)
0
1
2
3
4
5
6
7
8
T(C°) -40 -30 -20 -10 0 10 20 30
RH(%) 20 30 40 50 60 70 80 90 100

Figure 12

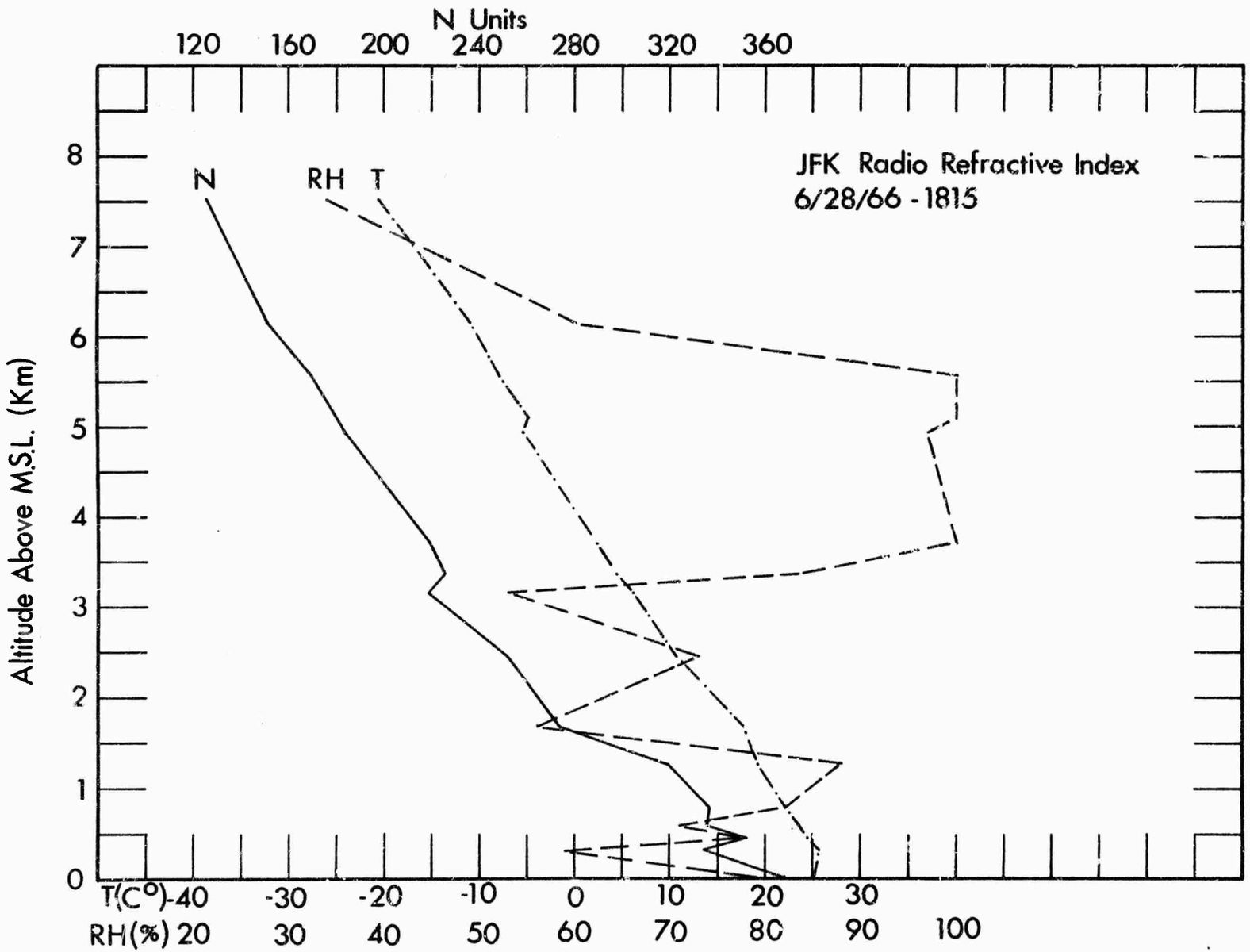
N Units
120
160
200
240
280
320
360
JFK Radio Refractive Index
6/28/66 - 1815
N
RH
T
Altitude Above M.S.L. (Km)
0
1
2
3
4
5
6
7
8
T(C°) -40 -30 -20 -10 0 10 20 30
RH(%) 20 30 40 50 60 70 80 90 100

Figure 13

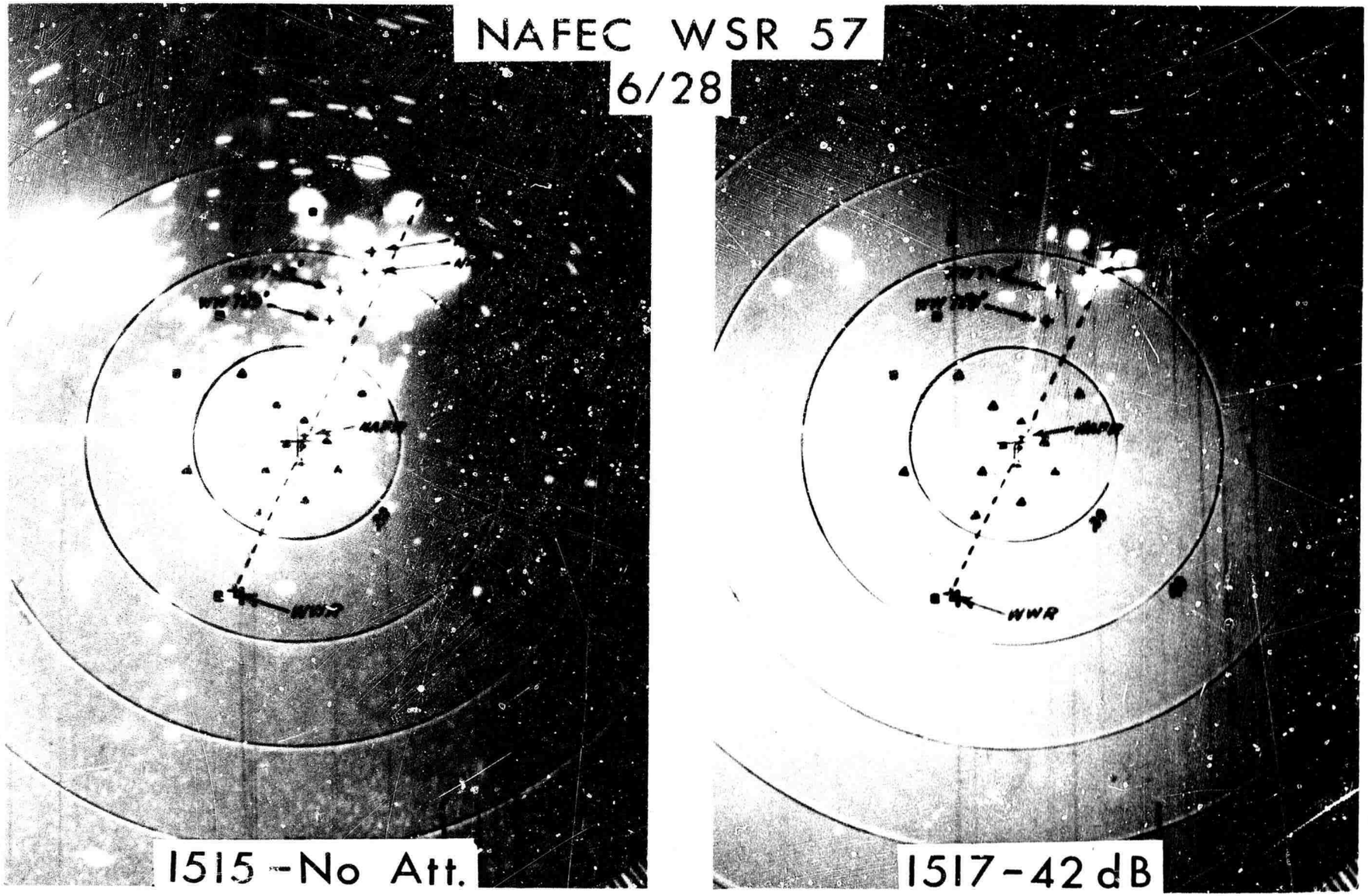

Figure 14

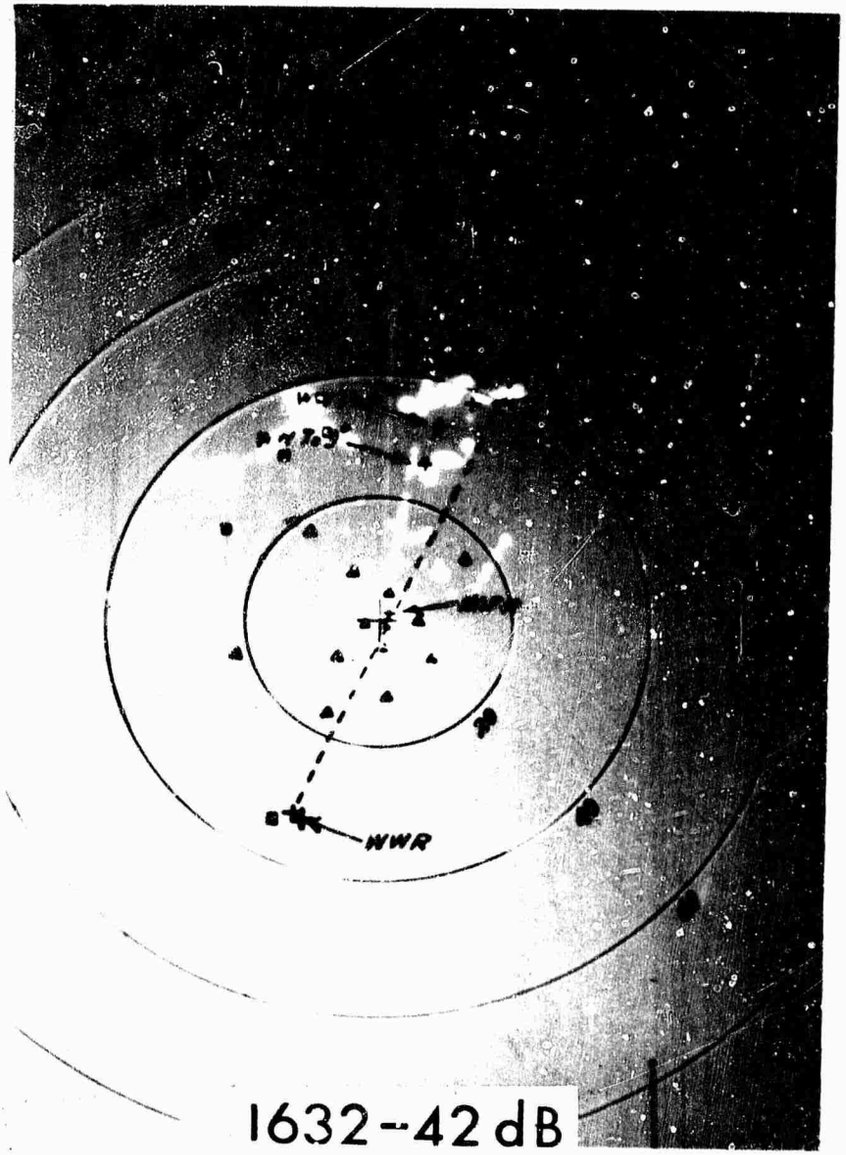

Figure 15

1708 – No Att.

1710 – 42 dB

Figure 16

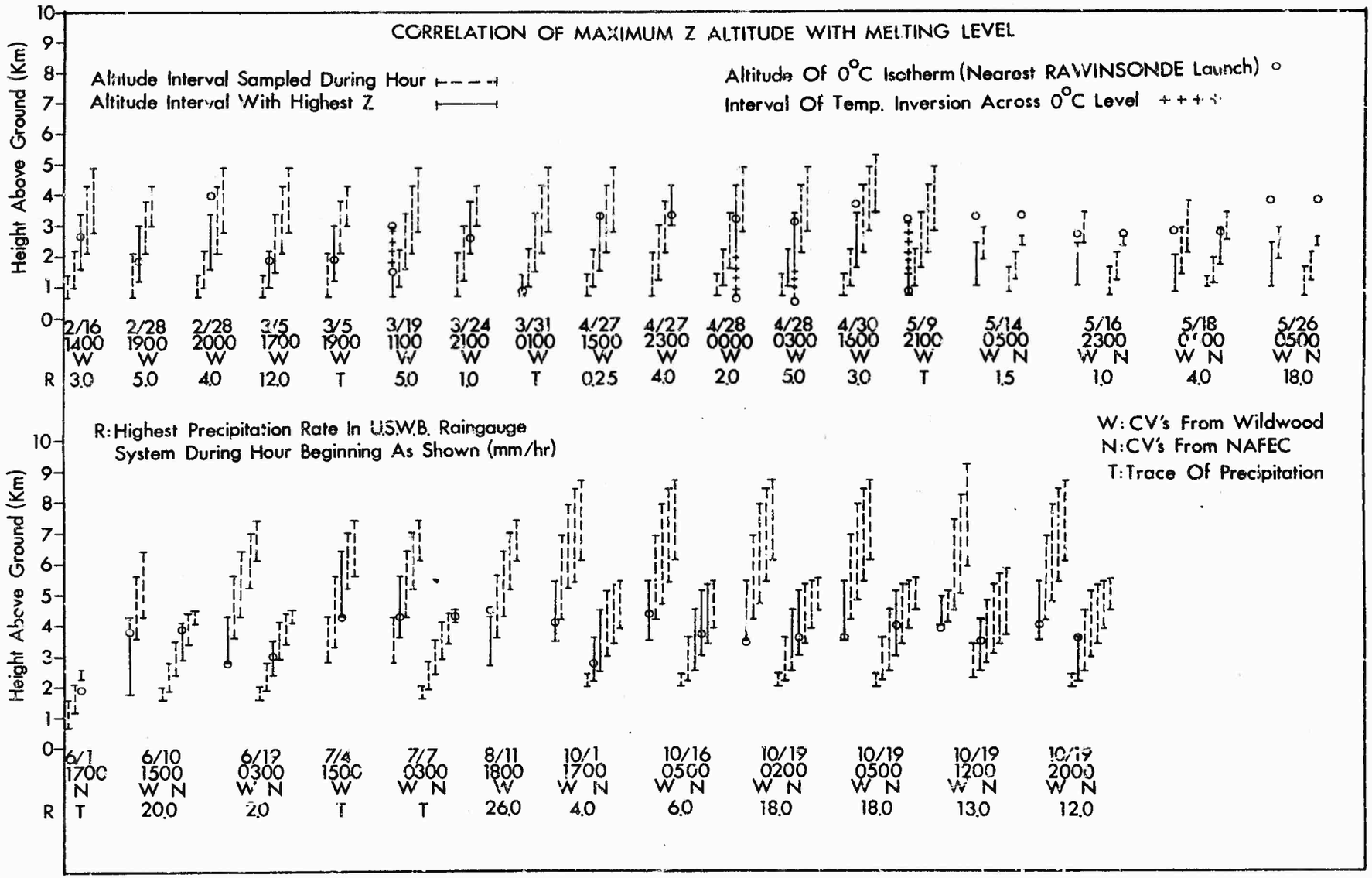
CORRELATION OF MAXIMUM Z ALTITUDE WITH MELTING LEVEL
Altitude Interval Sampled During Hour
Altitude Interval With Highest Z
Altitude Of 0°C Isotherm (Nearest RAWINSONDE Launch)
Interval Of Temp. Inversion Across 0°C Level
Height Above Ground (Km)
2/16 1400 W R 3.0
2/28 1900 W 5.0
2/28 2000 W 4.0
3/5 1700 W 12.0
3/5 1900 W T
3/19 1100 W 5.0
3/24 2100 W 1.0
3/31 0100 W T
4/27 1500 W 0.25
4/27 2300 W 4.0
4/28 0000 W 2.0
4/28 0300 W 5.0
4/30 1600 W 3.0
5/9 2100 W T
5/14 0500 W N 1.5
5/16 2300 W N 1.0
5/18 0100 W N 4.0
5/26 0500 W N 18.0
R: Highest Precipitation Rate In U.S.W.B. Raingauge System During Hour Beginning As Shown (mm/hr)
W: CV's From Wildwood
N: CV's From NAFEC
T: Trace Of Precipitation
6/1 1700 N R T
6/10 1500 W N 20.0
6/19 0300 W N 2.0
7/4 1500 W T
7/7 0300 W N T
8/11 1800 W 26.0
10/1 1700 W N 4.0
10/16 0500 W N 6.0
10/19 0200 W N 18.0
10/19 0500 W N 18.0
10/19 1200 W N 13.0
10/19 2000 W N 12.0

Figure 17

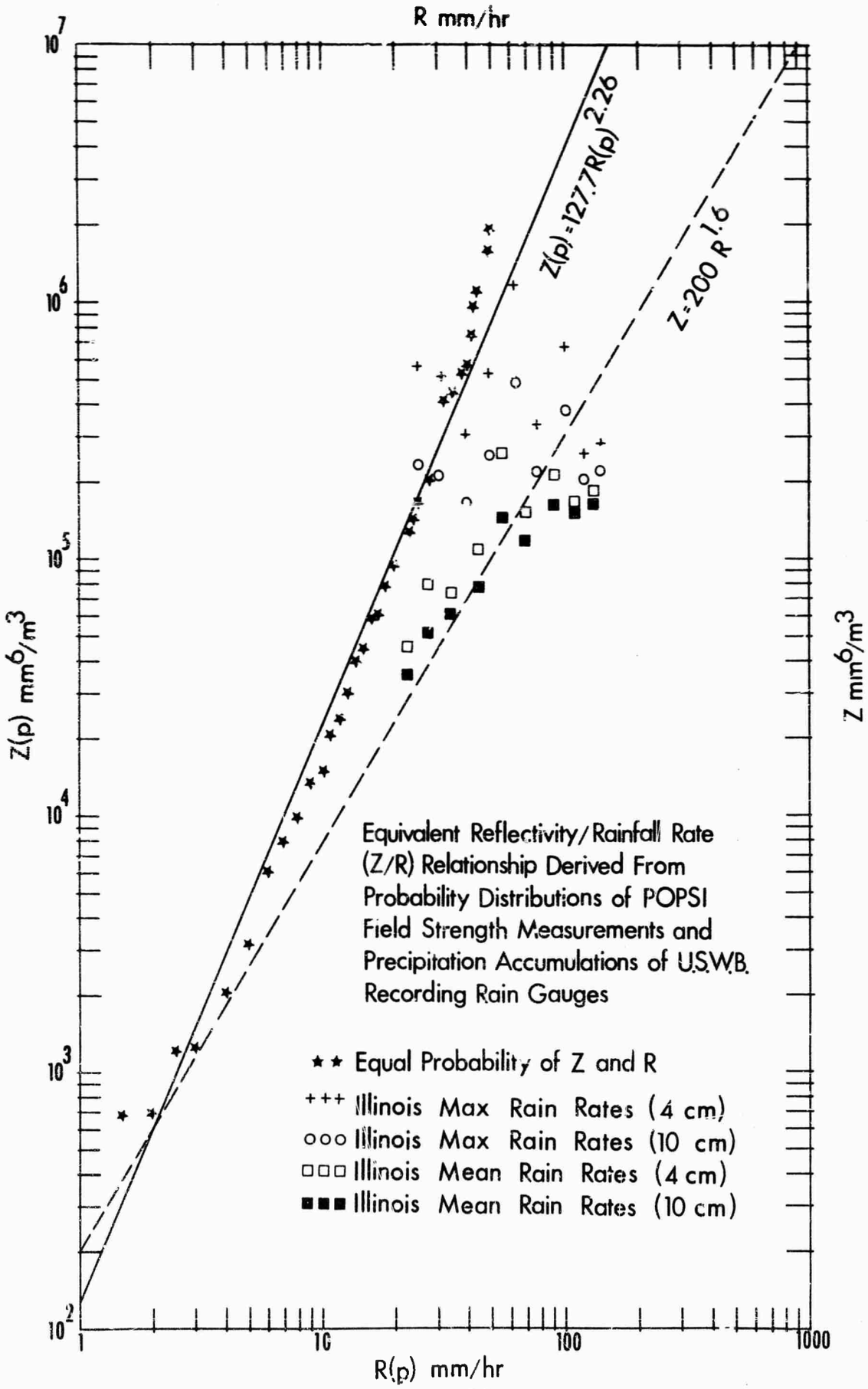
R mm/hr
10^7
10^6
10^5
10^4
10^3
10^2
Z(p) mm^6/m^3
Z mm^6/m^3
$Z(p) = 127.7 R(p)^{2.26}$
$Z = 200 R^{1.6}$
Equivalent Reflectivity/Rainfall Rate (Z/R) Relationship Derived From Probability Distributions of POPSI Field Strength Measurements and Precipitation Accumulations of U.S.W.B. Recording Rain Gauges
★★ Equal Probability of Z and R
+++ Illinois Max Rain Rates (4 cm)
ooo Illinois Max Rain Rates (10 cm)
□□□ Illinois Mean Rain Rates (4 cm)
■■■ Illinois Mean Rain Rates (10 cm)
1
10
100
1000
R(p) mm/hr

Figure 18

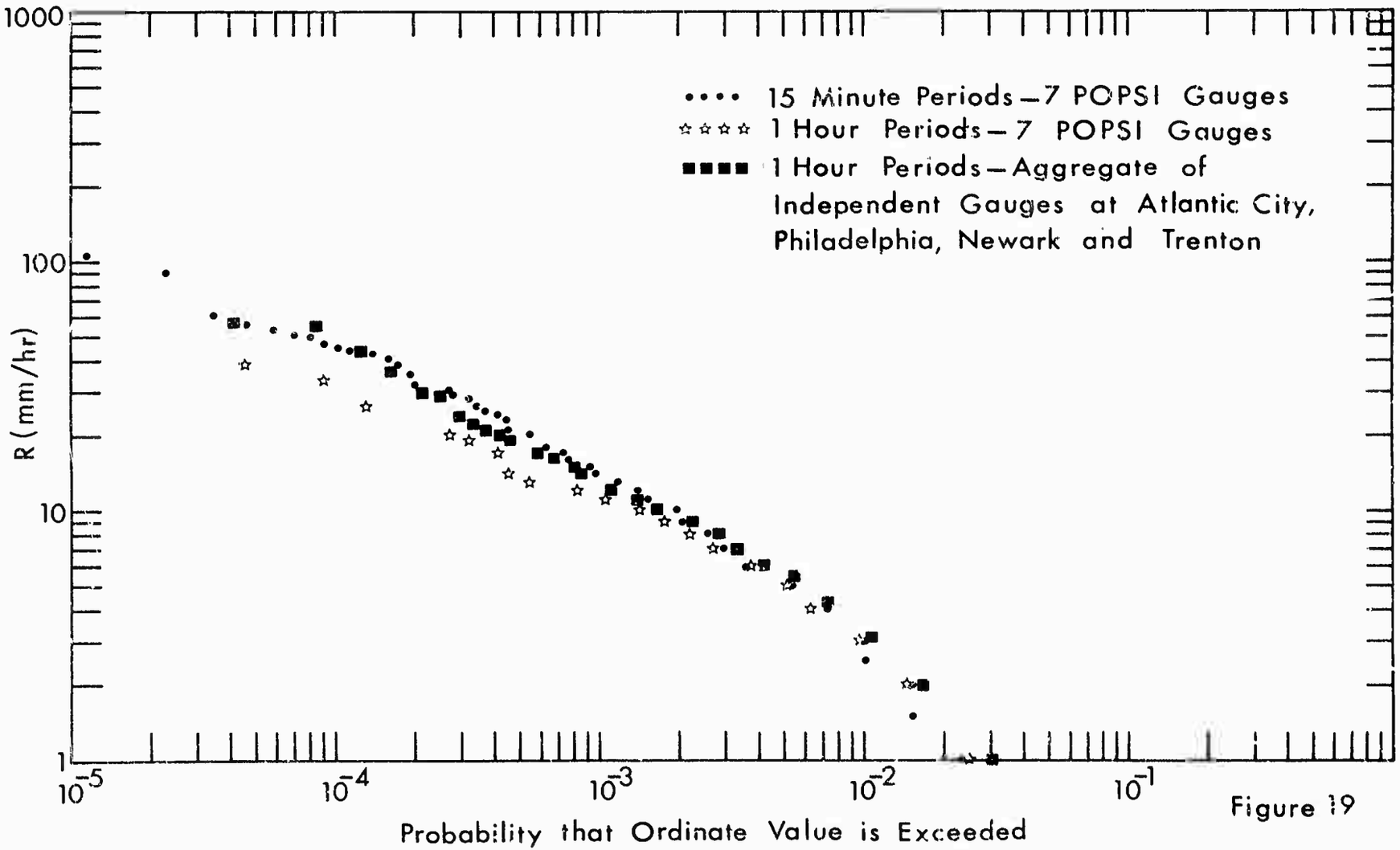
1000
100
10
1
R (mm/hr)
10^{-5}
10^{-4}
10^{-3}
10^{-2}
10^{-1}
Probability that Ordinate Value is Exceeded
15 Minute Periods—7 POPSI Gauges
1 Hour Periods—7 POPSI Gauges
1 Hour Periods—Aggregate of Independent Gauges at Atlantic City, Philadelphia, Newark and Trenton

Figure 19

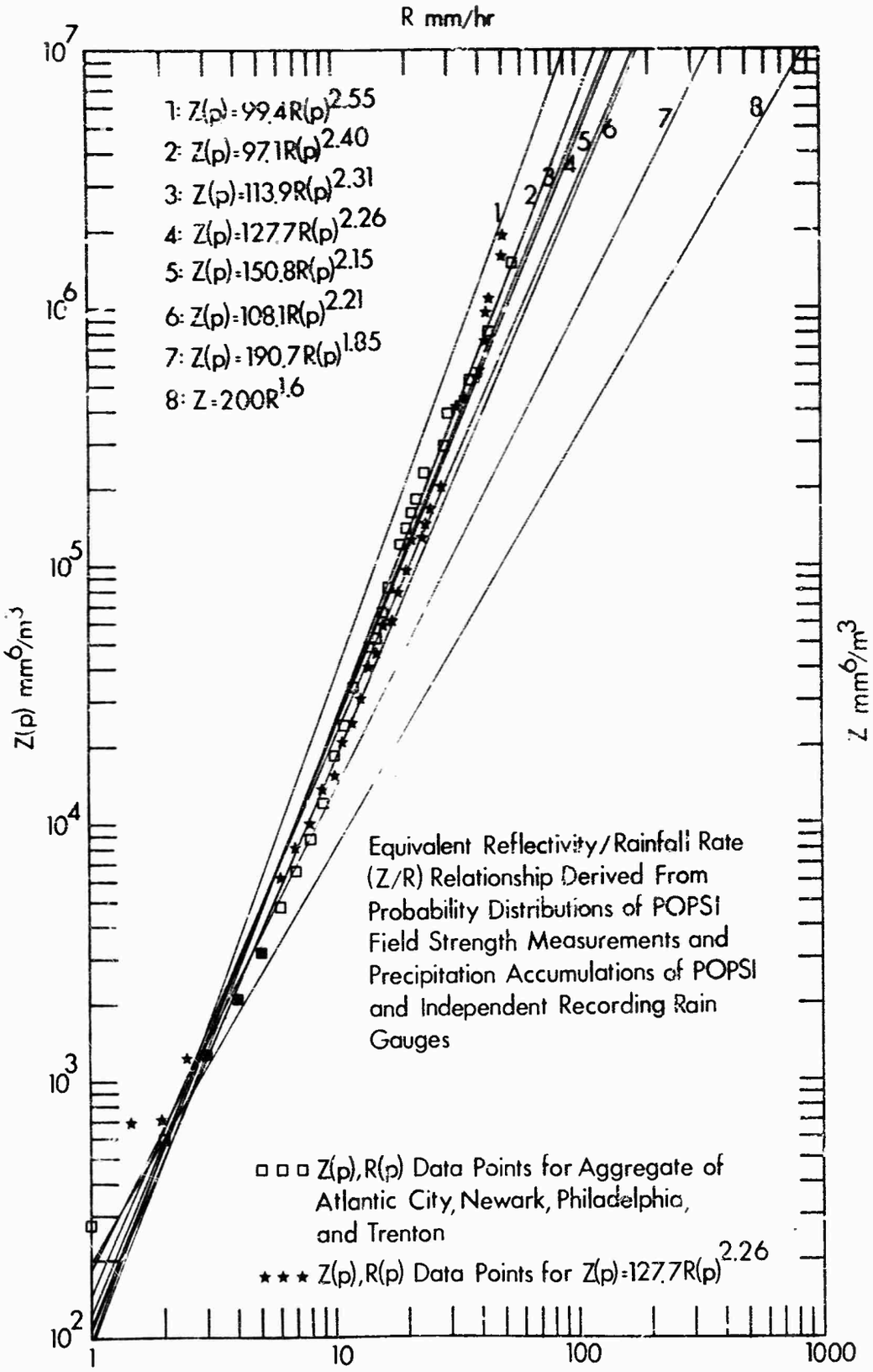
R mm/hr
1: Z(p)=99.4R(p)^2.55
2: Z(p)=97.1R(p)^2.40
3: Z(p)=113.9R(p)^2.31
4: Z(p)=127.7R(p)^2.26
5: Z(p)=150.8R(p)^2.15
6: Z(p)=108.1R(p)^2.21
7: Z(p)=190.7R(p)^1.85
8: Z=200R^1.6
Z(p) mm^6/m^3
Z mm^6/m^3
Equivalent Reflectivity/Rainfall Rate (Z/R) Relationship Derived From Probability Distributions of POPSI Field Strength Measurements and Precipitation Accumulations of POPSI and Independent Recording Rain Gauges
□ □ □ Z(p),R(p) Data Points for Aggregate of Atlantic City, Newark, Philadelphia, and Trenton
★ ★ ★ Z(p),R(p) Data Points for Z(p)=127.7R(p)^2.26
R(p) mm/hr

Figure 20